Chlamydia trachomatis restricts signaling through NOD2 until late in the pathogen's developmental cycle.

Grace Overman[1, 2], Iris Loeckener[3], Zachary Williford[1, 2], Sung Davis[1, 2], Aissata Diallo[1,2], Josie Blair[1,2], Beate Henrichfreise[3#], and George W. Liechti[1#]

[1] Department of Microbiology and Immunology, Uniformed Services University, Bethesda, MD, United States of America.

[2] Henry Jackson Foundation for the Advancement of Military Medicine, Bethesda, MD, United States of America.

[3] Institute for Pharmaceutical Microbiology, University of Bonn, Bonn, Germany.

#Corresponding Authors:

Department of Microbiology and Immunology, Uniformed Services University, 4301 Jones Bridge Road (B4100), Bethesda, MD. Tel: +1-301-295-8138 Email: george.liechti@usuhs.edu, bhenrich@uni-bonn.de

22 Key words: *Chlamydia*, Innate Immunity, peptidoglycan, NOD2, pathoadaptation,
23 persistence
24

ABSTRACT

Pathogenic chlamydial species restrict their peptidoglycan (PG) to the division septum of their replicative forms. PG is a microbe-associated molecular pattern (MAMP) and two of its major pattern recognition receptors in human cells are nucleotide-binding oligomerization domain-containing proteins 1 and 2 (NOD1 and NOD2, respectively). It has been proposed that this unique morphological feature is evidence of pathoadaptation by the microbe, permitting PG-dependent cell division while also reducing the bacterium's recognition by innate immune receptors. *Chlamydia trachomatis*-infected cells activate NOD1 signaling within 8-12 hours of exposure to the bacterium, roughly coinciding with the microbe's transition from its infectious to replicative forms. Here we report that, unlike NOD1 signaling, *Chlamydia*-induced NOD2 signaling does not occur until later in the pathogen's developmental cycle. Both *C. trachomatis* and the related murine pathogen *Chlamydia muridarum* signal late in infection in HEK293 reporter cell lines expressing either human or murine-derived NOD2 receptors. NOD2 signaling can be modulated by disruption of the chlamydial amidase enzyme, $AmiA_{CT}$, interrupting the microbe's developmental cycle, and treatment with inhibitors of lipooligosaccharide or peptidoglycan biosynthesis / assembly. These results mirror prior observations with Chlamydia-induced TLR9 signaling, leading us to hypothesize that Chlamydia-induced NOD2 signaling results from lytic events that occur sporadically during the transition between the pathogen's developmental forms. Given our finding that pre-treating cells with NOD2-stimulatory ligands reduces chlamydial inclusion size and delays the developmental cycle, we

47 hypothesize that the microbe preferentially degrades its PG during development to

48 reduce the generation of NOD2 ligands.

INTRODUCTION

Chlamydia trachomatis is the leading cause of bacterial sexually transmitted disease and infectious blindness in the world, with over 100 million estimated cases of sexually transmitted infection[1] and ~100 million people still at risk of trachoma-induced blindness[2]. This obligate, intracellular microbe has evolved a number of pathoadaptive means of circumventing the human immune system at the cellular level. Though this pathogen is susceptible to many commercial antibiotics, the estimated burden within the global population remains high due to the large majority of infections being asymptomatic[3,4], enabling the organism to spread in the absence of effective screening and treatment.

One of the adaptations made by chlamydial species to life inside of host organisms is the utilization of a biphasic developmental cycle[5]. Infectious forms, termed Elementary bodies (EBs) have reduced metabolic rates[6] and utilize lipooligosaccharide and gDNA with significantly reduced immunostimulatory properties[7-11]. Upon entering into host cells, chlamydial EBs transition into Reticulate bodies (RBs), and begin replicating via a unique cell division process[12] that is dependent on the synthesis and turnover of peptidoglycan (PG)[13-15]. In most other bacterial species, to include some chlamydial-related organisms[16], PG is a major component of the bacterial cell wall (termed a sacculus) that confers strength and rigidity to bacterial cells, while also allowing microbes to maintain or alter their overall shape[17-19]. Pathogenic chlamydial species lack sacculi, but synthesize PG at their division planes[13,15,20]. Paradoxically, because they lack FtsZ[21], the major organizer of septal PG in almost all bacterial species[22], they utilize the PG synthesis machinery primarily associated with sacculus

72 construction in other bacterial species[15,23-29]. While encoding two PG synthase
73 complexes primarily associated with either side-wall[30] or septal[31] PG biosynthesis, *C.*
74 *trachomatis* utilizes both to modulate the dimensions of its 'PG ring' during the initial and
75 terminal stages of its division process[32,33].

76 It has been proposed that the absence of PG sacculi in chlamydial species is
77 evidence of pathoadaptation by these organisms[13,15,34,35], due to PG being a major
78 immunostimulatory molecule that is recognized by a wide range of host cellular
79 receptors[36]. As PG is only present in the organism's replicative forms and in relatively
80 low abundance when compared to the amount required to generate sacculi, it stands to
81 reason that reducing the abundance of PG-derived muropeptides would directly impact
82 *Chlamydia*-host cell interaction(s). This hypothesis is supported in part by the
83 characterization of a rudimentary PG-recycling pathway encoded by *C. trachomatis* that
84 enables the reabsorption of meso-diaminopimelic acid (mDAP)– containing
85 muropeptides[37,38], further reducing its immunostimulatory profile.

86 The two most well-studied immunoreceptors for bacterial PG recognition are the
87 NOD-like receptors (NLRs) NOD1 and NOD2[39]. NOD1 recognizes PG-derived peptides
88 containing mDAP[40] while NOD2 primarily recognizes peptides containing N-
89 acetylmuramic acid (MurNAc), the principle component of NOD2 / CARD15 stimulatory
90 ligands[41]. While it has been over a decade since PG was first demonstrated to be
91 present in these organisms[13], the degree to which these receptors play a role during
92 Chlamydia infections is still in question[42]. Correlative studies examining patient cohorts
93 have noted an association between NOD1 functionality and bacterial clearance /
94 disease pathology[43,44] while a less robust association has been observed between

95 reduced NOD2 functionality and an increased risk of tubal pathology subsequent to
96 chlamydial infection[45]. Both receptors are expressed throughout the female reproductive
97 tract[46,47], with some evidence that expression of NOD2 (but not NOD1) is impacted by
98 phases of the menstrual cycle[48]. NOD1 induction has been demonstrated to have a
99 significant role in inducing inflammation in vitro[49-51], and murine studies have linked both
100 receptors to Endoplasmic Reticulum Stress-Induced Inflammation during chlamydial
101 infection and NOD1/2-deficient mice exhibit a reduction in clearance rates[52,53], though it
102 is presently unclear if these phenotypes are associated with ligand-dependent or ligand-
103 independent NOD1/2 signaling[54].

104 We have previously reported that PG can be visualized in cells infected with *C.*
105 *trachomatis* as early as 8 hours post-infection (hpi)[13], coinciding with the transition of
106 EBs to RBs and transcriptome data demonstrating the expression of chlamydial genes
107 associated with PG biosynthesis and turnover[55]. NOD1 signaling can be observed
108 within 24 hpi in cells infected with *C. trachomatis*, and we have previously demonstrated
109 that treatment with various antibiotics, metal chelators, and host cell cytokines can
110 impact the intensity of chlamydia-induced NOD1 signaling[56]. Interestingly, while NOD2-
111 stimulatory ligands have been reported to be present in lysates generated from
112 Chlamydia-infected cells[57], no signaling was observed 24 hpi when reporter cells were
113 infected directly, as noted by Packiam (personal communication, April 2014). Given our
114 recent work demonstrating that TLR9 signaling is delayed in Chlamydia-infected cells
115 and appears to be dependent on either bacterial lysis or transitioning between
116 chlamydial forms[9], we reasoned that this could potentially explain the discrepancy under

117 these two conditions. We set out to establish the dynamics of Chlamydia-induced NOD2

118 signaling, and determine what factor(s) impact its amplitude and temporal kinetics.

119 **RESULTS**

120 ***Chlamydia trachomatis* signals via NOD2 late in the pathogen's developmental**
121 **cycle.** We utilized a secreted embryonic alkaline phosphatase (SEAP) reporter system
122 to compare the relative signaling of human (h)NOD1 and hNOD2 in cells infected with
123 *C. trachomatis*. HEK-Blue cells stably express hNOD1 and hNOD2 and an NFκB-
124 inducible SEAP reporter gene. By comparing SEAP levels present in cell supernatants
125 between hNOD-expressing cells and cells lacking hNOD expression (Null1 and Null2
126 cells), NOD-specific signaling can be assessed between controls and a variety of
127 experimental conditions. SEAP was detected in the supernatants of *C. trachomatis*
128 infected cells at elevated levels at 24 and 44 hours post infection (hpi) for NOD1 (**Fig.**
129 **1A**), however, NOD2 signaling appeared to be delayed as SEAP was only present at
130 appreciable levels in cell supernatants at 44 hpi (**Fig. 1B**). In order to more closely
131 follow the kinetics of *C. trachomatis*-induced NOD2 signaling, we conducted real-time
132 monitoring of SEAP levels present in cell supernatants, beginning at 18hpi. Infected
133 cells were incubated in HEK-Blue Detection cell culture medium, allowing hydrolysis of
134 substrate by SEAP to be measured via microplate reader every 10 minutes for 28
135 hours. We found that SEAP begins to accumulate at detectable levels ~19-20 hpi and
136 that activity began to accelerate in a MOI-dependent manner at ~24 hpi (MOI ~2) and
137 ~30 hpi (MOI ~0.2) (**Fig. 1C**). As these observations roughly overlap with the
138 pathogen's transition from its replicative to infectious form, we concluded that NOD2
139 ligand release may be the result of *C. trachomatis* undergoing developmental form
140 conversion.
141

142 **Chlamydia-specific NOD2 signaling in HEK293 cells occurs as a result of**
143 **developmental form conversion.** We have previously reported that recognition of
144 chlamydial species by TLR9 also occurs late in infection, and we proposed that
145 chlamydial DNA is likely released due to random lytic events that occur during the
146 transition from RBs to EBs[9]. To test whether interrupting the developmental cycle could
147 prevent / dampen NOD2-stimulatory muropeptide release, we infected hNOD2 cells with
148 *C. trachomatis*, and added chloramphenicol at various time points post infection to
149 interrupt protein synthesis and subsequently prevent developmental form conversion.
150 When protein synthesis was inhibited at 18 hpi, a time point prior to developmental form
151 conversion[58], NOD2 signaling decreased, and slowly increased when chloramphenicol
152 was added at later and later time points (**Fig. 2A**). By contrast, when chlamydial LOS
153 biosynthesis was inhibited with the use of a LpxC inhibitor (LPC-011[59,60]), NOD2
154 signaling was significantly increased when higher MOIs were used **(Fig. 2B)**. This
155 enhancement did not appear to significantly impact the timing of NOD2-ligand release,
156 as signaling was only observed at the 44hpi time point and only when higher MOIs were
157 used. These observations, in addition to the kinetics of Chlamydia-specific NOD2
158 signaling **(Fig 1C)**, support the premise that NOD2 ligand release from *C. trachomatis* is
159 likely a result of developmental form conversion.
160
161 **Knock-down of *amiA$_{Ct}$* impacts NOD2 signaling.** Assuming that bacterial lysis is the
162 cause for the release of NOD2-stimulatory ligands in Chlamydia-infected cells, it is not
163 readily apparent why the release of Chlamydia-specific, NOD1-stimulatory ligands is not
164 similarly impacted. As mentioned previously, *C. trachomatis* encodes a rudimentary

165 peptidoglycan recycling pathway that enables it to limit the amount of meso-DAP-
166 containing peptidoglycan fragment release into the intracellular environment[37,38],
167 however, to date no pathway for the recycling of anhydroMurNAc has been
168 characterized in any Chlamydia species.

169 We questioned whether the molecular process(es) of PG degradation employed
170 by the pathogen potentially influence its NLR stimulatory potential. *C. trachomatis* and
171 other *Chlamydia spp*. and chlamydia-related organisms make use of two separate
172 degradation enzymes in order to remodel their septal PG during the initiation and
173 termination of their division process: an amidase (AmiA) that cleaves the stem peptide
174 from MurNAc[61] and a lytic transglycosylase (SpoIID) that cleaves denuded glycan
175 strands[62]. MurNAc alone is a poor stimulator of NOD2 receptors, and most stimulatory
176 ligands require at least two amino acids of the PG stem peptide to be present, in the
177 correct spatial isomerism, in order for MurNAc to bind sufficiently well to result in a
178 signaling cascade[63]. We reasoned that under normal conditions inherent to the PG
179 turnover found in *Chlamydia* species, sufficient amidase activity would effectively
180 eliminate any and all amino acids attached to MurNAc, thus fundamentally skewing NLR
181 signaling towards NOD1 (which is mDAP-specific[40]) and away from NOD2.

182 In order to assess the impact of the chlamydial amidase on NOD2 signaling, we
183 utilized a previously characterized CRISPRi-knockdown approach[64] in order to gauge
184 how reducing amidase activity would impact NOD signaling in *C. trachomatis*-infected
185 cells. *C. trachomatis* strain -pL2 was transformed with either an empty plasmid; pLCria
186 (NT), a knockdown construct; pLCria (*amiA*), or a knockdown construct with a HIS-
187 tagged complementation allele; pLCria-amiA_6xHIS (amiA) (Dannenberg *et al*., in prep).

188 Each strain was then titered and used to infect hNOD2-expressing HEK293 reporter
189 cells under either native or inducing conditions. Counter to our initial hypothesis, the
190 transformant containing the AmiA knockdown plasmid appeared to exhibit slightly
191 enhanced baseline NOD2 signaling when compared to control strains, a trend that
192 reached statistical significance when higher MOIs were used (**Fig. 3A, left column**).
193 When the three strains were compared using the lower MOI, the AmiA knockdown
194 strain exhibited a significant ($p \leq 0.0001$) decrease in NOD2 signaling (**Fig. 3B, right**
195 **column**), a result that did not reach significance in either empty vector or
196 complementation control strains.
197
198 **Inducers of persistence enhance Chlamydia-specific NOD2 signaling.** Under
199 stress-inducing conditions, chlamydial species are capable of entering a state of
200 persistence in which their replicative forms stop dividing, and the developmental cycle
201 will effective pause until the stress-inducing condition is lifted, after which the microbe
202 will resume dividing and transition into its infectious form[65]. There is considerable
203 debate as to whether this aberrant / persistent state is physiologically relevant in the
204 context of active infections[65-71]. We have previously proposed that one of the defining
205 characteristics of this state should be the degree to which it impacts host-microbial
206 interactions at the cellular level[56]. Numerous studies have demonstrated that inducing
207 chlamydial persistence can directly impact the recognition of the organism by various
208 TLRs and NLRs[9,56,72,73]. Given that chlamydia-induced NOD1-signaling has been
209 demonstrated to be impacted in persistently infected cells[56], we reasoned that NOD2
210 would be similarly impacted. Upon the addition of D-cycloserine and ampicillin, which

211 respectively inhibit peptidoglycan precursor synthesis[74,75] and assembly[76], we found that
212 NOD2 signaling in *C. trachomatis*-infected cells was significantly enhanced **(Fig. 4)**. D-
213 cycloserine was particularly impactful, as NOD2 signaling was observed in DCS-treated,
214 *C. trachomatis*-infected cells as early as 24 hpi and was enhanced as well at later time
215 points **(Fig. 4A)**. When NOD2 signaling was tracked over the span of the chlamydial
216 developmental cycle, signaling from DCS-treated cells began diverging from control and
217 other treatment groups ~23-24 hpi, while ampicillin-treated cells diverged at ~38 hpi
218 **(Fig. 4B)**. We also observed enhanced NOD2 signaling in cells that were treated with
219 the iron chelator 2,2′-bipyridyl. Overall, these results demonstrate that induction of
220 aberrance / persistence with the use of PG-targeting antibiotics and iron chelators can
221 significantly impact the degree and kinetics of chlamydia-induced NOD2 signaling.
222
223 **Pre-treatment of NOD-expressing cells impacts the development of *C.***
224 ***trachomatis*.** Given the difference in signaling kinetics observed between NOD1 and
225 NOD2-expressing HEK293 cells infected with *C. trachomatis* and *C. muridarum*, we
226 wanted to examine whether the resulting signaling cascades adversely impact the
227 growth / development of *C. trachomatis* under native expression conditions. We pre-
228 treated HepG2 cells, which have been previously shown to express both NOD1[77] and
229 NOD2[78], with ligands that stimulate NOD1 (L-Ala-γ-D-Glu-mDAP; Tri-DAP) or NOD2
230 (muramyl dipeptide; MDP) and subsequently infected them with *C. trachomatis* at an
231 MOI of ~4. At 24 hpi, we then fixed cells and labeled them with antiserum raised against
232 the chlamydial Major Outer Membrane Protein (MOMP). Inclusion numbers were
233 roughly equivalent between all control and test groups examined (data not shown),

234 indicating that NOD-stimulation did not appear to adversely impact inclusion formation.
235 When all MOMP-labeling data was assessed we found cells that were pretreated with
236 MDP prior to infection exhibited smaller inclusion sizes when compared to untreated,
237 Tri-DAP, and MDP + Tri-DAP-treated conditions **(Fig. 5)**. We repeated this assay in two
238 additional cell lines originally derived from cervical (C-33A) and uterine (SiHa) tissue
239 and found that all treatment groups reduced the average inclusion size at 24 hpi.
240 We subsequently utilized an inclusion-forming unit (IFU) assay to assess the
241 impact of pre-treatment with NOD1 and NOD2 stimulatory ligands on the chlamydial
242 developmental cycle. We examined the development of *C. trachomatis* L2 strain 434 Bu
243 in HepG2, C-33A, and SiHa cells by assessing the number of viable EBs recoverable at
244 various time points in the pathogen's developmental cycle. In HepG2 cells, we
245 recovered significantly fewer EBs 48 hours post-infection in the MDP-pretreated group,
246 but these differences were absent when IFUs were recovered at 72 hpi (**Fig. 6A**). We
247 observed similar results in both MDP pretreated C-33A ($p \leq 0.002$) and SiHa ($p \leq 0.17$)
248 cells **(Fig. 6B,C)** indicating that pre-treatment with PG-derived muropeptides delays
249 chlamydial development in multiple tissue culture cell lines.
250
251 ***Both hNOD2 and mNOD2 recognize C. trachomatis and C. muridarum-specific***
252 ***muropeptides.*** To conclude this study, we set out to determine whether NOD2
253 signaling kinetics in Chlamydia-infected cells was unique to i) the human pathogen
254 and/or ii) the human NOD2 receptor. Subsequent experiments were carried out in
255 tandem comparing the NOD2-stimulatory potential of *C. trachomatis* with the murine
256 pathogen *Chlamydia muridarum*. We found that, like *C. trachomatis*, *C. muridarum*-

257 induced hNOD2 expression also appeared to exhibit delayed signaling (**Fig. 7A**).
258 Interestingly, *C. muridarum* also appeared to induce hNOD2 to a greater extent than *C.*
259 *trachomatis*. We hypothesized that this heightened signaling from *C. muridarum* might
260 be due to one of two factors: differences in the rates of replication between the two
261 pathogens[79] and / or differences in how each pathogen's PG was recognized by
262 hNOD2. To test these two non-exclusive possibilities, we replicated our signaling study
263 in HEK 293 cells expressing the murine version of the NOD2 receptor (mNOD2). Both
264 pathogens exhibited similar kinetics in mNOD2 signaling, with SEAP activity only
265 observable at the 44 hpi time point (**Fig. 7B**). Surprisingly, *C. trachomatis* induced
266 higher signaling than *C. muridarum* in mNOD2-expressing cells, potentially indicating
267 that species-specific recognition, rather than differences in bacterial replication rates, is
268 the driving force behind observed differences in NOD2 signaling between these two
269 species.

270 **DISCUSSION**

271 We have presented data indicating that NOD1 and NOD2 signaling in
272 Chlamydia-infected cells is temporally distinct, and that the kinetics of signaling appear
273 to be impacted by the mechanism(s) the organism utilizes to degrade its PG-derived
274 muropeptides. While these differences appear to be significant, their potential impact on
275 chlamydial development *in vitro* and *in vivo* is less clear. One potential impact of altering
276 NLR signaling might be modulating signaling cascades in such a manner as to be
277 beneficial to the pathogen. While NLRs are associated with upregulation of various
278 cytokine responses[80], many of which are prevalent during chlamydial infections[81], one
279 notable difference between NOD1/2 signaling involves a process of direct relevance to
280 most intracellular pathogens: autophagy. NOD2$^{-/-}$ mice exhibit hypersensitivity to viruses
281 as a result of defects in autophagy, specifically mitophagy, resulting in NLRP3
282 inflammasome activation and the generation of enhanced levels of IL-18[82]. Conversely,
283 chlamydia-infected cells demonstrate the promotion of autophagy[83-85] and the inhibition
284 of apoptosis[86-89]. While autophagy has been demonstrated to occur in Chlamydia-
285 infected cells in culture, significant levels are generally not observable until later in
286 chlamydial development[83] and defects in autophagy have been demonstrated to
287 enhance chlamydial growth[84,85]. Given our observation that pre-treatment with NOD2-
288 stimulatory ligands slows chlamydial development in multiple cell lines, we hypothesize
289 that the delayed release of NOD2-stimulatory ligands by *C. trachomatis* represents a
290 pathoadaptation by the microbe, potentially limiting cellular autophagy early in its
291 developmental cycle.

292 NOD2 is generally thought to enhance cellular autophagy through ATG16L1 in a
293 PI3K, ATG5, and ATG7-dependent manner[90]. ATG16L1 has been shown to restrict the
294 expansion of the chlamydial inclusion, but is re-directed by the secreted chlamydial
295 protein CT622/TaiP to enable vesicular traffic to the inclusion[91]. Given that we see a
296 reduction in inclusion size in MDP pre-treated cells **(Fig. 5)**, it is tempting to speculate
297 that NOD2 signaling impacts chlamydial development by recruiting the majority of
298 cellular ATG16L1 towards autophagy, thus leaving less free to be utilized by TaiP to
299 recruit vesicular traffic to the growing chlamydial inclusion. The regulation of NOD2-
300 stimulatory ligands by chlamydial species may also exhibit tissue-specific effects, as
301 MDP has recently been shown to increase oxidative respiration and ATP production
302 while decreasing oxidative stress in human intestinal epithelial cells[92]. Experiments
303 investigating these interesting possibilities are currently ongoing.

304 Many of our observations in this study mirrored those previously reported regarding
305 *Chlamydia*-induced TLR9 signaling[9]. Both *Chlamydia*-induced NOD2 and TLR9
306 signaling occur late in infection, can be significantly reduced if protein synthesis is
307 inhibited prior to phase conversion, and are significantly enhanced when infected cells
308 are treated with inhibitors of either PG or LOS biosynthesis. Given that PG and LOS
309 inhibitors are known to interrupt phase conversion and impact the integrity of the
310 bacterial membrane, we hypothesize that their presence results in an increase in
311 chlamydial lytic events, resulting in PG and gDNA release. The observation that *C.*
312 *muridarum* and *C. trachomatis* appear to differ in the intensity of their signaling in a
313 host-specific manner is another notable finding. While both hNOD2 and mNOD2
314 recognize MDP and both have similar downstream signaling pathways, some

315 differences have been observed such as the degree to which mutant alleles are capable
316 of suppressing IL-10 expression[93]. Species-specific differences have been noted for
317 other TLRs and NLRs with regard to their regulation, ligand specificity and function[94],
318 and differences in ligand specificity and sensitivity have been previously demonstrated
319 for both hNOD1 and mNOD1[95].

320 As persistence in *Chlamydia* species often leads to a disruption in membrane
321 integrity[96], we were not surprised by the finding that NOD2 levels increased significantly
322 as a result of persistence induction. Our observation of enhanced NOD2 signaling in
323 cells that were treated with the iron chelator 2,2′-bipyridyl was unexpected, as this
324 condition has previously been demonstrated to significantly reduce chlamydia-specific
325 NOD1 signaling at early infection time points[56]. The finding that DCS substantially
326 impacts not only the degree but also the timing of Chlamydia-specific NOD2 signaling
327 was particularly interesting. This observation matches those previously made
328 investigating Chlamydia-derived, NOD2-stimulatory ligands present in HeLa cell
329 lysates[57], indicating that the enhancement is not simply a result of the sonication steps
330 involved in preparing the material for evaluation. DCS is a D-alanine analog, originally
331 isolated from *Streptomyces*[97,98], and historically its mechanism of action has been
332 understood to be the result of it competitively binding to D-alanine racemase; Alr[75] and
333 D-alanine-D-alanine ligase; Ddl[99]. Chlamydia species lack canonical Alr and DadX
334 homologs, but encode GlyA enzymes capable of D-Ala racemase activity, which is also
335 inhibited by DCS[100]. The inactivation of these two enzymes should inhibit PG
336 biosynthesis. As chlamydial species do not encode MpaA homologs that would normally
337 function to hydrolyze γ-D-glutamyl-diaminopimelic acid[101], the result of treatment should

338 be the accumulation of UDP-MurNAc-L-Ala-D-Glu-*meso*-DAP (UDP-MTP) in the
339 chlamydial cytoplasm. While muramyl tripeptide (MTP) is not well recognized by
340 NOD2[95], the presence of a Uridine Diphosphate (UDP) carrier group in the PG
341 precursor molecule (UDP-MTP) substantially enhances its recognition by NOD2
342 receptors[102]. This would support the hypothesis that NOD2 signaling from DCS-treated
343 Chlamydia-infected cells is likely due to the release of PG-precursors (namely UDP-
344 MTP) by aberrant RBs. Given that UDP-MTP is normally localized to the bacterial
345 cytoplasm, this would appear to indicate that chlamydial RBs under these conditions are
346 undergoing appreciable levels of cellular lysis. Alternatively, it has been recently
347 suggested that DCS is capable of being utilized as a substrate by both L,D- and D,D-
348 transpeptidases and is capable of being incorporated into the stem peptide of PG at the
349 4th and 5th position, respectively[103]. It is presently unclear whether these DCS-containing
350 peptide stems are capable of being crosslinked, or whether their presence significantly
351 impacts immunorecognition by NLRs.
352 The chlamydial amidase $AmiA_{CT}$ appears to meaningfully impact Chlamydia-
353 induced NOD2 signaling (**Fig 3**). During PG turnover, $AmiA_{CT}$ cleaves stem peptides
354 from MurNAc[61], and only once this has occurred can lytic transglycosylases (ie.
355 $SpoIID_{CT}$) bind to and subsequently degrade the newly denuded PG glycan stands.
356 However, we have also shown that disruptions in chlamydial membrane integrity,
357 alterations in PG biosynthesis, and chlamydial lytic events that can occur during phase
358 conversion can all influence chlamydial-derived NOD2 signaling. The enhanced
359 background signaling and slightly enlarged RBs present in our uninduced, $AmiA_{CT}$
360 knockdown strain would appear to indicate low levels of dCAS9 expression. When

361 baseline NOD2 levels are equivalent between all three strains when using a lower MOI,
362 we see a significant decrease in NOD2 signaling upon induction specific to our
363 knockdown strain **(Fig. 3B)**. Assuming that SpoIID$_{CT}$ is unable to process glycan
364 strands prior to amidase activity, it is somewhat puzzling that the knockdown of amidase
365 activity would impact NOD2 activity. As we observe elevated NOD2 signaling at higher
366 MOIS and lower activity under induction conditions at lower MOIs, we speculate that
367 this data may represent different origins of NOD2-stimulatory ligands and potentially
368 support the hypothesis that PG fragments are not the principle NOD2-stimulatory
369 ligands being released by *C. trachomatis*. Given our DCS-treatment data (**Fig. 4**), we
370 conclude that PG-precursors that still retain their UDP carrier motif likely make up a
371 substantial portion of the NOD2-stimulatory ligands present in Chlamydia-infected cells,
372 though subsequent experimentation will be needed to further validate this.
373 While this study effectively demonstrates potential differences in the temporal
374 kinetics of Chlamydia-induced NOD1 and NOD2 signaling, it is important to point out
375 that these phenotypes will almost certainly differ in hematopoietic vs. non-hematopoietic
376 cell types. While *C. trachomatis* may effectively delay NOD2 signaling until late in
377 development by cleaving stem peptides during the natural PG degradative processes
378 associated with its division cycle, this may not significantly impact the production of
379 NOD2-stimulatory PG fragments generated by cellular responses to infection, such as
380 the potential degradation of RBs within lysosomal compartments within hematopoietic
381 cells **(Fig. 7)**. However, as only chlamydial RBs synthesize and maintain PG[13,15], its
382 availability for NOD1/2 interactions in immune cells would largely depend on the kinetics
383 of the pathogen trafficking to lysosomes. Given that the EB-to-RB transition occurs

384 roughly 8 to 12 hpi, this is presumably plenty of time for EB-containing vesicles to traffic
385 to lysosomes[104,105]. It is tempting to speculate that the origins of EB-to-RB transition
386 kinetics may have arisen, in part, as a means of dampening potential immune
387 responses generated in hematopoietic cells that are incompatible with chlamydial
388 replication and development. Alternatively, as the major NOD2-stimulatory ligand (MDP)
389 is a known activator of NALP3/NLRP3[106], its release during RB degradation could
390 contribute to neutrophil killing via NLRP3 inflammasome[107]. Work investigating how the
391 timing of inclusion-lysosomal fusion impacts these downstream processes in a cell-type
392 specific manner is currently under active investigation.
393

394 **CONCLUSIONS**

395 In this study, we demonstrate that chlamydia infection can be detected by both
396 NOD1 and NOD2 receptors *in vitro*, but that the kinetics of that signaling differs
397 significantly with NOD2 signaling lagging behind that of NOD1. Additionally, we
398 effectively demonstrate that the timing and intensity of NOD2 signaling can be impacted
399 by a variety of factors: chlamydial / host species, incidence of chlamydial lysis, the
400 relative activity of the chlamydial amidase enzyme, and the induction of aberrance /
401 'persistence' phenotypes. Our results strongly suggest that chlamydial PG precursors,
402 rather than degraded PG fragments, are the primary stimulators of NOD2. Given our
403 observations that pre-stimulating host cells with MDP delays chlamydial development
404 and NOD2's unique association with cellular autophagy induction, we reason that the
405 delay in NOD2-induction by chlamydial species directly benefits the development of
406 these obligate, intracellular pathogens.

407 **MATERIALS AND METHODS**

408 **Reagents:**

409 Anti-MOMP antisera (LS-C123239) was purchased from LSBio. LpxC inhibitor LPC-011
410 was graciously provided by Dr. Pei Zhou (Duke University). Muramyl dipeptide (MDP)
411 and L-Ala-γ-D-Glu-mDAP (Tri-DAP) were purchased from InvivoGen.

412

413 **Bacterial Strains and Cell Lines:**

414 *C. trachomatis* serovar L2 strain 434/Bu, *C. muridarum* strain Nigg, and *E. coli* strain
415 MG1655 were provided by Anthony Maurelli (University of Florida). *C. trachomatis* and
416 *C. muridarum* stocks were generated utilizing HeLa-USU cells (also provided by
417 Anthony Maurelli) unless otherwise noted. *C. trachomatis* strains -pL2 transformed with
418 pLCria (NT), pLCria (*amiA*), and pLCria-amiA_6xHIS (amiA) vectors were provided by
419 Scot Ouellette (University of Nebraska Medical Center) and are characterized in
420 Dannenberg *et al*. (manuscript in prep). Whole cell lysate ('crude') freezer stocks of *C.*
421 *trachomatis* and *C. muridarum* EBs were generated from HeLa cells 40 hours post
422 infection and stored at -80° C in sucrose phosphate glutamic acid buffer (7.5% w/v
423 sucrose, 17 mM Na_2HPO_4, 3 mM NaH_2PO_4, 5 mM L-glutamic acid, pH 7.4) until
424 use. Stocks were titered via inclusion forming unit (IFU) assay (described below). HEK-
425 Blue-hNOD1, -hNOD2, -mNOD2, and -Null1 cells were purchased from InvivoGen and
426 propagated according to the manufacturer's instructions. Cell lines were passaged in
427 high-glucose Dulbecco's modified Eagle medium (DMEM; Gibco) and 10% fetal bovine
428 serum (FBS; HyClone). HepG2 cells were purchased from ATCC and propagated
429 according to their instructions. All cell lines were checked for mycoplasma

430 contamination 2 passages after the initial liquid nitrogen thaw, and every subsequent 10
431 passages.
432
433 **HEK-Blue hNOD2, mNOD2, Null1 and Null2 NF-κB reporter assay:** HEK-Blue cells
434 expressing human or murine NOD2 and carrying the NF-κB SEAP (secreted embryonic
435 alkaline phosphatase) reporter gene (InvivoGen) were used according to the
436 manufacturer's instructions and adapted to assess NLR-specific NF-κB activity induced
437 via live *C. trachomatis* and *C. muridarum*. Briefly, 3×10^5 cells/ml were plated in 96-well
438 plates (total reaction volume of 200 µl per well [~6.0×10^4 cells per well]) and allowed to
439 settle/adhere overnight at 37°C. Media was then removed and replaced with 200 µl of
440 medium containing either *C. trachomatis* or *C. muridarum* (at the MOIs indicated) or
441 known NOD-stimulatory ligands (triDAP and MDP). For experiments examining the
442 impact of conditionally enhancing the developmental cycle of *Chlamydia* spp. on NOD
443 signaling, multiple MOIs were used. Plates were then centrifuged for 1 h at 2,000 × *g*
444 and subsequently incubated in a CO_2 incubator at 37°C. Cell supernatants were
445 collected at indicated time points for subsequent analysis of SEAP activity. A
446 colorimetric reporter assay was then utilized to quantify the abundance of SEAP in cell
447 supernatants. Twenty microliters of supernatant collected from infected cells was added
448 to 180 µl of the SEAP detection solution (InvivoGen), followed by incubation at 37°C for
449 ~6 h. SEAP enzymatic activity was then quantified using a plate reader set to 650 nm.
450 Infected cells were compared to uninfected cells (negative control) and cells treated with
451 triDAP / MDP (positive controls). To ensure that changes in alkaline phosphatase
452 activity were NLR-dependent under each of the experimental conditions tested, all

453 experiments were carried out in parallel in either HEK-Blue-Null1 or HEK-Blue-Null2 cell
454 lines, which contains empty expression vectors but lack NOD1/2. Each HEK-Blue SEAP
455 reporter assays was always carried out in three separate experiments, statistical
456 analysis was conducted by either 1- or 2-way ANOVA, and significance values were
457 analyzed by utilizing Sidak's multiple-comparison test. For real-time tracking of NOD2
458 signaling, hNOD2 reporter cells were plated, and infected as described above, but
459 instead of DMEM / 10% FBS, cells were incubated in HEK-Blue Detection cell culture
460 medium. Plates were placed in a Stratus microplate reader (Cerillo), which itself was
461 placed in a CO_2 incubator at 37°C. OD650 readouts were obtained beginning at 18hpi
462 every 10 minutes for the subsequent 28 hours.
463
464 ***C. trachomatis* Infections of HepG2, C-33A, and SiHa cells:** ~2.5 x 10^5 cells / mL
465 were spun down and resuspended in infection medium containing ~1x10^6 IFU of *C.*
466 *trachomatis* (MOI ~4). A MOI of 4 was used in order to maximize the number of
467 inclusions visible per field of view. 2.5 x 10^5 cells were then added to each well of a 24
468 well plate and placed in the incubator for 24 or 44 hours. For pre-stimulation
469 experiments, ~2.5 x 10^5 cells / mL were spun down and resuspended in infection
470 medium + / - 20 µg/mL triDAP, 20 µg/mL muramyl dipeptide (MDP), or 10 ug/mL of
471 each and incubated overnight at 37° C. The next morning, cells were spun down and
472 resuspended in infection medium containing ~1x10^6 IFU of *C. trachomatis* (MOI ~4), 2.5
473 x 10^5 cells were then added to each well of a 24 well plate and placed in the incubator
474 (at 37° C). Cells were then either fixed for inclusion visualization or lysed for the
475 enumeration of viable EBs via IFU assay.

476

477 **Fluorescence Microscopy / MOMP-labeling:** Briefly, HeLa cells were infected with *C.*
478 *trachomatis* L2 434/Bu as described above. A MOI of 4 was used, in order to ensure a
479 higher number of visible MOMP-containing objects within a single imaging field. At
480 indicated time points infection medium was removed, and cells were washed three
481 times with 1× PBS. Cells were fixed and permeabilized with methanol for 5 min and
482 gently washed three times with 1× PBS. Cells were then further permeabilized and
483 blocked as described above. Cells were then incubated with anti-MOMP (1:500) for 1
484 hour at room temperature, followed by several washes in 3% BSA, and subsequent
485 incubation with anti-goat conjugated antibodies (1:1000 Alexa594). For visualizing cell
486 nuclei, cells were incubated with Hoechst stain for ~10 min and then washed with 3%
487 BSA and 1× PBS. Coverslips were mounted on slides with ProLong gold antifade
488 mounting medium and stored in the dark at 4°C prior to imaging via structured-
489 illumination (Elyra PS.1) microscopy. For inclusion size measurements, imaging was
490 conducted on a Zeiss 980 confocal microscope. zStacks were acquired at random for
491 ~10 fields of view per condition, and inclusion volume dimensions were calculated
492 utilizing the 3D object counter addon (ImagJ / Fiji).

493

494 **Inclusion-forming Unit (IFU) Assay:** Viable EBs were assessed as previously
495 described[9]. Briefly, 96-well tissue culture-treated plates were seeded 24 hours prior to
496 infection with ~40,000 cells per well. On the day of infections, bacterial suspensions
497 from crude cell lysates were thawed on ice, and serially diluted in DMEM / 10% FBS +
498 0.5 ug/mL cycloheximide. Spent media was removed from each well and 200 µl of each

499 chlamydia dilution was added to each well. Plates were then centrifuged at 3000 x g at
500 35° C for 1 hour, then incubated at 37° C with 5% CO2 for an additional 23 hours. Cells
501 were then fixed with ice cold methanol for 10 minutes, washed with 3 x PBS, blocked
502 with 3% BSA for 1 hour, incubated with goat anti-MOMP (LSBio) for 1 hour at RT,
503 washed 3 x with PBS, incubated with donkey anti-goat Alexa Fluor 488 (Invivogen) for 1
504 hour at RT, and washed 3 x with PBS. Plates were then examined under an
505 epifluorescence microscope (Olympus) within 24 hours. Total inclusion forming units
506 (IFU) were calculated by counting the number of visible inclusions for 10 different
507 imaging fields (per condition) using the 40x objective.
508
509 **Data Availability:** All data generated in this manuscript will be made available without
510 restriction upon request. This includes all super resolution imaging data, all reporter cell
511 line SEAP data, and chlamydial IFU calculations.

512 **ACKNOWLEDGEMENTS**

513 We would like to thank Dr. Anthony Maurelli (University of Florida) and his laboratory for
514 providing us with the strains used in this work as well as helpful feedback during the
515 development of this project. We would like to thank Dr. Scot Ouellette (UNMC) for
516 providing us with strains for conducting the $AmiA_{CT}$ knockdown experiments. We would
517 also like to thank Dr. Pei Zhou (Duke University) for graciously providing us with the
518 LpxC inhibitor used in this work. This work was supported by a MIRA ESI award (R35
519 GM138202) and a USU faculty start up award (HP73LIEC18) to GL. Funding was also
520 provided by the Deutsche Forschungsgemeinschaft (DFG, German Research
521 Foundation), project-ID 398967434 —TRR261 (BH) and 390536577 (BH), and the
522 funding scheme FEMHABIL, Medical Faculty, University of Bonn (BH). The funders had
523 no role in study design, data collection and interpretation, or the decision to submit the
524 work for publication. The opinions and assertions expressed herein are those of the
525 author(s) and do not necessarily reflect the official policy or position of the Uniformed
526 Services University or the Department of Defense.

527

528 **AUTHOR CONTRIBUTIONS**

529 Conceptualization and Design, IL, BH, GL; Data Curation and Formal analysis, GO, IL,
530 ZW, SD, AD, and GL; Investigation, Methodology, Validation, Visualization, IL, AD, GO,
531 ZW, JB, and GL, Writing – original draft, GL; Writing – review & editing, GO, IL, ZW, SD,
532 JB, BH, and GL; Funding acquisition, Project administration and Supervision, BH and
533 GL. All authors read and approved the final manuscript.

534

DECLARATION OF INTERESTS

The authors declare that no competing interests exist.

537 **FIGURE LEGENDS**

538 **Figure 1. *Chlamydia trachomatis* signals via NOD2 late in the pathogen's**
539 **developmental cycle.** SEAP activity was measured from the supernatants of hNOD1
540 **(A)** and hNOD2 **(B)** and Null1/2 HEK 293 reporter cells infected with *C. trachomatis*
541 serovar L2 (strain Bu/434) at 24 and 44 hpi. Data points represent separate, biological
542 replicates, with lines delineating the mean and error bars representing the standard
543 error of the mean. Groups were compared via one-way ANOVA with multiple
544 comparisons. ****; $p \leq 0.0001$, ns; not significant. **(C)** SEAP activity was measured in
545 the supernatants of infected NOD2-expressing HEK 293 reporter cells grown in HEK-
546 Blue™ Detection media. OD_{650} values for each well were assessed every ten minutes
547 beginning at 18 hpi, and values plotted are relative to mock infected control wells on the
548 same plate. Data is representative of three wells per condition on the same plate
549 (technical replicates). Positive control (muramyl dipeptide; MDP) was added to control
550 wells at 18 hpi.

551

552 **Figure 2. Chlamydia-specific NOD2 signaling in HEK293 cells occurs as a result**
553 **of developmental form conversion. (A)** *C. trachomatis*-infected hNOD2-HEK293
554 reporter cells were treated with chloramphenicol (25 ug/mL; Cam_{25}) at the time points
555 indicated and SEAP activity was measured at 44hpi. **(B,C)** The effects of the LOS
556 inhibitor LPC-011 on *C. trachomatis*-induced NOD2 signaling at 24 **(B)** and 44 **(C)** hpi.
557 Data points represent three independent, biological replicates and error bars represent
558 standard error of the mean. Groups were compared via two-way ANOVA with multiple
559 comparisons. ****; $p \leq 0.0001$, **; $p \leq 0.01$, *; $p \leq 0.05$, ns, not significant.

560

561 **Figure 3. Knockdown of *amiA*$_{ct}$ impacts NOD2 signaling at lower MOIs.** hNOD2-
562 expressing HEK293 SEAP reporter cells were infected with *C. trachomatis* strains at
563 MOIs of 2 and 0.2 containing either pLCria (NT), pLCria (*aimA*), or pLCria-amiA_6xHIS
564 (*amiA*). Infections were carried out in the presence / absence of 1nM aTc and
565 supernatants were tested for the presence for SEAP activity 48 hpi. Data points
566 represent three biological replicates, lines indicate the mean of those replicates, and
567 error bars represent standard error of the mean. Groups were compared via two-way
568 ANOVA with multiple comparisons. ****; $p \leq 0.0001$, ns, not significant. Data are
569 presented as comparisons between strains **(A)** and between conditions **(B)**.

570

571 **Figure 4. Inducers of persistence enhance Chlamydia-specific NOD2 signaling.**
572 **(A)** SEAP activity was measured from the supernatants of hNOD2 and Null2 HEK 293
573 reporter cells infected with *C. trachomatis* serovar L2 (strain Bu/434) in the presence /
574 absence of antibiotics that target the assembly (ampicillin) and biosynthesis (D-
575 cycloserine; DCS) of peptidoglycan at 24 and 44 hpi. Data points indicate individual
576 biological replicates, lines delineate the mean of those replicates, and error bars
577 represent standard error of the mean. Groups were compared via two-way ANOVA with
578 multiple comparisons. ****; $p \leq 0.0001$, **; $p \leq 0.01$, *; $p \leq 0.05$, ns; not significant. **(B)**
579 SEAP activity was measured in the supernatants of infected NOD2-expressing HEK 293
580 reporter cells grown in HEK-Blue™ Detection media in the presence / absence of
581 peptidoglycan-targeting antibiotics (ampicillin, DCS), and the iron-chelator 2'2 bipyridyl.
582 OD_{650} values for each well were assessed every ten minutes beginning at 18 hpi, and

583 values plotted are relative to mock infected control wells on the same plate. Data is
584 representative of three technical replicates per group.
585
586 **Figure 5. Pre-treatment with NOD1- and NOD2-stimulatory ligands prior to**
587 **infection with *C. trachomatis* significantly impacts inclusion size in NLR-**
588 **expressing cell lines.** HepG2, C-33A, and SiHa cells were pretreated with Tri-DAP,
589 muramyl dipeptide (MDP), or both, prior to infection with *C. trachomatis* L2 strain
590 Bu/434. At 24 hpi, cells were fixed, inclusions were labeled, counted, and measured.
591 zStacks of MOMP-labeled objects were obtained from a Zeiss 700 confocal microscope
592 and approximate volume measurements were calculated for all inclusions present within
593 10 imaging fields. Data presented represent all MOMP-labeled objects counted resulting
594 in inclusions > 20 μm^3; 3 µm across with red lines indicating the mean of each group
595 within a dataset. Significance was assessed via 1-way ANOVA with multiple
596 comparisons. ****; $p \leq 0.0001$, ***; $p \leq 0.001$, *; $p \leq 0.05$, ns; not significant.
597
598 **Figure 6. Pre-treatment with NOD2-stimulatory ligands delays the development of**
599 ***C. trachomatis* in NLR-expressing cell lines.** HepG2 **(A)**, C-33A **(B)**, and SiHa **(C)**
600 cells were either left untreated or pre-treated with the NOD1-stimulatory ligand Tri-DAP,
601 the NOD2-stimulatory ligand MDP, or both Tri-DAP and MDP. After 24 hours, cells were
602 infected with *C. trachomatis* and the development of infectious EBs was assessed at the
603 indicated time points (30, 48, and 72 hpi). Lines delineate the mean of 3 separate
604 biological replicates with each replicate displayed as a colored dot. Significance was

605 assessed via 1-way ANOVA with multiple comparisons. **; $p \leq 0.01$, *; $p \leq 0.05$, ns; not
606 significant.
607
608 **Figure 7. Both hNOD2 and mNOD2 recognize *C. trachomatis* and *C. muridarum*-**
609 **specific muropeptides.** SEAP activity was measured from the supernatants of hNOD2
610 **(A)**, mNOD2 **(B)**, and Null2 HEK 293 reporter cells infected with *C. trachomatis* serovar
611 L2 (strain Bu/434) at 24 and 44 hpi. Data points represent separate, biological
612 replicates, lines delineate the mean, and error bars represent standard error of the
613 mean. Groups were compared via one-way ANOVA with multiple comparisons. ****; $p \leq$
614 0.0001, ***; $p \leq 0.001$, **; $p \leq 0.01$, *; $p \leq 0.05$, ns, not significant.
615
616 **Figure 8. NOD2 signaling as a function of chlamydial lysis during the**
617 **developmental cycle and 'persistence'. (A)** During normal developmental conditions,
618 the chlamydial inclusion avoids fusing with lysosomal compartments in the host cell.
619 After RB conversion, the degradation of PG by $AmiA_{CT}$ during chlamydial replication
620 results in the release of NOD1-stimulatory peptides. Lytic events triggered by
621 developmental form conversion or 'persistence' inducers result in the release of partially
622 degraded PG as well as PG precursors, which activate NOD2 signaling. **(B)** In cases
623 were the chlamydial inclusion fuses with lysosomes (such as in phagocytic cells) at later
624 timepoints in the microbe's developmental cycle (> 8 hpi), we hypothesize that RBs are
625 degraded and NOD2-stimulatory ligands released at a higher abundance, potentially
626 leading to alterations in inflammasome activation.

627 **REFERENCES**

628 1 Newman, L. *et al.* Global Estimates of the Prevalence and Incidence of Four Curable
629 Sexually Transmitted Infections in 2012 Based on Systematic Review and Global
630 Reporting. *PLoS One* **10**, e0143304 (2015). https://doi.org/10.1371/journal.pone.0143304
631 2 Organization, W. H. WHO Alliance for the Global Elimination of Trachoma: progress
632 report on elimination of trachoma, 2023. 363-380 (2024).
633 3 Price, M. J. *et al.* The natural history of Chlamydia trachomatis infection in women: a
634 multi-parameter evidence synthesis. *Health Technol Assess* **20**, 1-250 (2016).
635 https://doi.org/10.3310/hta20220
636 4 Farley, T. A., Cohen, D. A. & Elkins, W. Asymptomatic sexually transmitted diseases:
637 the case for screening. *Prev Med* **36**, 502-509 (2003). https://doi.org/10.1016/s0091-
638 7435(02)00058-0
639 5 Elwell, C., Mirrashidi, K. & Engel, J. Chlamydia cell biology and pathogenesis. *Nat Rev*
640 *Microbiol* **14**, 385-400 (2016). https://doi.org/10.1038/nrmicro.2016.30
641 6 Omsland, A., Sager, J., Nair, V., Sturdevant, D. E. & Hackstadt, T. Developmental stage-
642 specific metabolic and transcriptional activity of Chlamydia trachomatis in an axenic
643 medium. *Proceedings of the National Academy of Sciences of the United States of*
644 *America* **109**, 19781-19785 (2012). https://doi.org/10.1073/pnas.1212831109
645 7 Ingalls, R. R. *et al.* The inflammatory cytokine response to Chlamydia trachomatis
646 infection is endotoxin mediated. *Infect Immun* **63**, 3125-3130 (1995).
647 https://doi.org/10.1128/iai.63.8.3125-3130.1995
648 8 Yang, C. *et al.* Chlamydia trachomatis Lipopolysaccharide Evades the Canonical and
649 Noncanonical Inflammatory Pathways To Subvert Innate Immunity. *mBio* **10** (2019).
650 https://doi.org/10.1128/mBio.00595-19
651 9 Diallo, A., Overman, G., Sah, P. & Liechti, G. W. Recognition of Chlamydia trachomatis
652 by Toll-like receptor 9 is altered during persistence. *Infect Immun* **92**, e0006324 (2024).
653 https://doi.org/10.1128/iai.00063-24
654 10 Ouburg, S. *et al.* TLR9 KO mice, haplotypes and CPG indices in Chlamydia trachomatis
655 infection. *Drugs Today (Barc)* **45 Suppl B**, 83-93 (2009).
656 11 Singer, M., de Waaij, D. J., Morre, S. A. & Ouburg, S. CpG DNA analysis of bacterial
657 STDs. *BMC Infect Dis* **15**, 273 (2015). https://doi.org/10.1186/s12879-015-1016-7
658 12 Abdelrahman, Y., Ouellette, S. P., Belland, R. J. & Cox, J. V. Polarized Cell Division of
659 Chlamydia trachomatis. *PLoS Pathog* **12**, e1005822 (2016).
660 https://doi.org/10.1371/journal.ppat.1005822
661 13 Liechti, G. W. *et al.* A new metabolic cell-wall labelling method reveals peptidoglycan in
662 *Chlamydia trachomatis*. *Nature* **506**, 507-510 (2014).
663 https://doi.org/10.1038/nature12892
664 14 Jacquier, N., Viollier, P. H. & Greub, G. The role of peptidoglycan in chlamydial cell
665 division: towards resolving the chlamydial anomaly. *FEMS Microbiol Rev* **39**, 262-275
666 (2015). https://doi.org/10.1093/femsre/fuv001
667 15 Liechti, G. *et al.* Pathogenic Chlamydia Lack a Classical Sacculus but Synthesize a
668 Narrow, Mid-cell Peptidoglycan Ring, Regulated by MreB, for Cell Division. *PLoS*
669 *Pathog* **12**, e1005590 (2016). https://doi.org/10.1371/journal.ppat.1005590

670 16 Pilhofer, M. *et al.* Discovery of chlamydial peptidoglycan reveals bacteria with murein
671 sacculi but without FtsZ. *Nat Commun* **4**, 2856 (2013).
672 https://doi.org/10.1038/ncomms3856
673 17 Navarro, P. P. *et al.* Cell wall synthesis and remodelling dynamics determine division site
674 architecture and cell shape in Escherichia coli. *Nat Microbiol* **7**, 1621-1634 (2022).
675 https://doi.org/10.1038/s41564-022-01210-z
676 18 Turner, R. D., Hurd, A. F., Cadby, A., Hobbs, J. K. & Foster, S. J. Cell wall elongation
677 mode in Gram-negative bacteria is determined by peptidoglycan architecture. *Nat*
678 *Commun* **4**, 1496 (2013). https://doi.org/10.1038/ncomms2503
679 19 Wang, S., Furchtgott, L., Huang, K. C. & Shaevitz, J. W. Helical insertion of
680 peptidoglycan produces chiral ordering of the bacterial cell wall. *Proceedings of the*
681 *National Academy of Sciences of the United States of America* **109**, E595-604 (2012).
682 https://doi.org/10.1073/pnas.1117132109
683 20 Brown, W. J. & Rockey, D. D. Identification of an antigen localized to an apparent
684 septum within dividing chlamydiae. *Infect Immun* **68**, 708-715 (2000).
685 https://doi.org/10.1128/IAI.68.2.708-715.2000
686 21 Ouellette, S. P., Lee, J. & Cox, J. V. Division without Binary Fission: Cell Division in the
687 FtsZ-Less Chlamydia. *J Bacteriol* **202** (2020). https://doi.org/10.1128/JB.00252-20
688 22 Barrows, J. M. & Goley, E. D. FtsZ dynamics in bacterial division: What, how, and why?
689 *Curr Opin Cell Biol* **68**, 163-172 (2021). https://doi.org/10.1016/j.ceb.2020.10.013
690 23 Gaballah, A., Kloeckner, A., Otten, C., Sahl, H. G. & Henrichfreise, B. Functional
691 analysis of the cytoskeleton protein MreB from Chlamydophila pneumoniae. *PLoS One*
692 **6**, e25129 (2011). https://doi.org/10.1371/journal.pone.0025129
693 24 Ouellette, S. P., Karimova, G., Subtil, A. & Ladant, D. Chlamydia co-opts the rod shape-
694 determining proteins MreB and Pbp2 for cell division. *Mol Microbiol* **85**, 164-178
695 (2012). https://doi.org/10.1111/j.1365-2958.2012.08100.x
696 25 Ouellette, S. P. *et al.* Analysis of MreB interactors in Chlamydia reveals a RodZ homolog
697 but fails to detect an interaction with MraY. *Front Microbiol* **5**, 279 (2014).
698 https://doi.org/10.3389/fmicb.2014.00279
699 26 Jacquier, N., Frandi, A., Pillonel, T., Viollier, P. H. & Greub, G. Cell wall precursors are
700 required to organize the chlamydial division septum. *Nat Commun* **5**, 3578 (2014).
701 https://doi.org/10.1038/ncomms4578
702 27 Kemege, K. E. *et al.* Chlamydia trachomatis protein CT009 is a structural and functional
703 homolog to the key morphogenesis component RodZ and interacts with division septal
704 plane localized MreB. *Mol Microbiol* **95**, 365-382 (2015).
705 https://doi.org/10.1111/mmi.12855
706 28 Ouellette, S. P., Rueden, K. J., AbdelRahman, Y. M., Cox, J. V. & Belland, R. J.
707 Identification and Partial Characterization of Potential FtsL and FtsQ Homologs of
708 Chlamydia. *Front Microbiol* **6**, 1264 (2015). https://doi.org/10.3389/fmicb.2015.01264
709 29 Harpring, M., Lee, J., Zhong, G., Ouellette, S. P. & Cox, J. V. FtsK is Critical for the
710 Assembly of the Unique Divisome Complex of the FtsZ-less Chlamydia trachomatis.
711 *bioRxiv* (2025). https://doi.org/10.1101/2024.10.24.620021
712 30 Meeske, A. J. *et al.* SEDS proteins are a widespread family of bacterial cell wall
713 polymerases. *Nature* **537**, 634-638 (2016). https://doi.org/10.1038/nature19331

714 31 Taguchi, A. *et al.* FtsW is a peptidoglycan polymerase that is functional only in complex
715 with its cognate penicillin-binding protein. *Nat Microbiol* **4**, 587-594 (2019).
716 https://doi.org/10.1038/s41564-018-0345-x
717 32 Cox, J. V., Abdelrahman, Y. M. & Ouellette, S. P. Penicillin-binding proteins regulate
718 multiple steps in the polarized cell division process of Chlamydia. *Sci Rep* **10**, 12588
719 (2020). https://doi.org/10.1038/s41598-020-69397-x
720 33 Liechti, G. W. Localized Peptidoglycan Biosynthesis in Chlamydia trachomatis
721 Conforms to the Polarized Division and Cell Size Reduction Developmental Models.
722 *Front Microbiol* **12**, 733850 (2021). https://doi.org/10.3389/fmicb.2021.733850
723 34 Wong, W. F., Chambers, J. P., Gupta, R. & Arulanandam, B. P. Chlamydia and Its Many
724 Ways of Escaping the Host Immune System. *J Pathog* **2019**, 8604958 (2019).
725 https://doi.org/10.1155/2019/8604958
726 35 Chen, H., Wen, Y. & Li, Z. Clear Victory for Chlamydia: The Subversion of Host Innate
727 Immunity. *Front Microbiol* **10**, 1412 (2019). https://doi.org/10.3389/fmicb.2019.01412
728 36 Wolf, A. J. & Underhill, D. M. Peptidoglycan recognition by the innate immune system.
729 *Nat Rev Immunol* **18**, 243-254 (2018). https://doi.org/10.1038/nri.2017.136
730 37 Singh, R., Liechti, G., Slade, J. A. & Maurelli, A. T. Chlamydia trachomatis Oligopeptide
731 Transporter Performs Dual Functions of Oligopeptide Transport and Peptidoglycan
732 Recycling. *Infect Immun* **88** (2020). https://doi.org/10.1128/IAI.00086-20
733 38 Reuter, J. *et al.* An NlpC/P60 protein catalyzes a key step in peptidoglycan recycling at
734 the intersection of energy recovery, cell division and immune evasion in the intracellular
735 pathogen Chlamydia trachomatis. *PLoS Pathog* **19**, e1011047 (2023).
736 https://doi.org/10.1371/journal.ppat.1011047
737 39 Franchi, L., Warner, N., Viani, K. & Nunez, G. Function of Nod-like receptors in
738 microbial recognition and host defense. *Immunol Rev* **227**, 106-128 (2009).
739 https://doi.org/10.1111/j.1600-065X.2008.00734.x
740 40 Girardin, S. E. *et al.* Nod1 detects a unique muropeptide from gram-negative bacterial
741 peptidoglycan. *Science* **300**, 1584-1587 (2003). https://doi.org/10.1126/science.1084677
742 41 Girardin, S. E. *et al.* Nod2 is a general sensor of peptidoglycan through muramyl
743 dipeptide (MDP) detection. *J Biol Chem* **278**, 8869-8872 (2003).
744 https://doi.org/10.1074/jbc.C200651200
745 42 Zou, Y., Lei, W., He, Z. & Li, Z. The role of NOD1 and NOD2 in host defense against
746 chlamydial infection. *FEMS Microbiol Lett* **363** (2016).
747 https://doi.org/10.1093/femsle/fnw170
748 43 Brankovic, I. *et al.* NOD1 in contrast to NOD2 functional polymorphism influence
749 Chlamydia trachomatis infection and the risk of tubal factor infertility. *Pathog Dis* **73**, 1-
750 9 (2015). https://doi.org/10.1093/femspd/ftu028
751 44 Jukema, J. B. *et al.* Can Previous Associations of Single Nucleotide Polymorphisms in
752 the TLR2, NOD1, CXCR5, and IL10 Genes in the Susceptibility to and Severity of
753 Chlamydia trachomatis Infections Be Confirmed? *Pathogens* **10** (2021).
754 https://doi.org/10.3390/pathogens10010048
755 45 den Hartog, J. E. *et al.* Do host genetic traits in the bacterial sensing system play a role in
756 the development of Chlamydia trachomatis-associated tubal pathology in subfertile
757 women? *BMC Infect Dis* **6**, 122 (2006). https://doi.org/10.1186/1471-2334-6-122

758 46 Hart, K. M. *et al.* Functional expression of pattern recognition receptors in tissues of the
759 human female reproductive tract. *J Reprod Immunol* **80**, 33-40 (2009).
760 https://doi.org/10.1016/j.jri.2008.12.004
761 47 Hafner, L. M., Cunningham, K. & Beagley, K. W. Ovarian steroid hormones: effects on
762 immune responses and Chlamydia trachomatis infections of the female genital tract.
763 *Mucosal Immunol* **6**, 859-875 (2013). https://doi.org/10.1038/mi.2013.46
764 48 Lebedeva, O. P. The role of NOD1 and NOD2 receptors in recognizing pathogens in the
765 female reproductive tract. *Obstetrics and Gynecology*, 25-29 (2019).
766 49 Buchholz, K. R. & Stephens, R. S. The cytosolic pattern recognition receptor NOD1
767 induces inflammatory interleukin-8 during Chlamydia trachomatis infection. *Infect*
768 *Immun* **76**, 3150-3155 (2008). https://doi.org/10.1128/IAI.00104-08
769 50 Opitz, B. *et al.* Nod1-mediated endothelial cell activation by Chlamydophila pneumoniae.
770 *Circ Res* **96**, 319-326 (2005). https://doi.org/10.1161/01.RES.0000155721.83594.2c
771 51 Welter-Stahl, L. *et al.* Stimulation of the cytosolic receptor for peptidoglycan, Nod1, by
772 infection with Chlamydia trachomatis or Chlamydia muridarum. *Cell Microbiol* **8**, 1047-
773 1057 (2006). https://doi.org/10.1111/j.1462-5822.2006.00686.x
774 52 Pham, O. H. *et al.* NOD1/NOD2 and RIP2 Regulate Endoplasmic Reticulum Stress-
775 Induced Inflammation during Chlamydia Infection. *mBio* **11** (2020).
776 https://doi.org/10.1128/mBio.00979-20
777 53 Shimada, K. *et al.* The NOD/RIP2 pathway is essential for host defenses against
778 Chlamydophila pneumoniae lung infection. *PLoS Pathog* **5**, e1000379 (2009).
779 https://doi.org/10.1371/journal.ppat.1000379
780 54 Keestra-Gounder, A. M. *et al.* NOD1 and NOD2 signalling links ER stress with
781 inflammation. *Nature* **532**, 394-397 (2016). https://doi.org/10.1038/nature17631
782 55 Belland, R. J. *et al.* Genomic transcriptional profiling of the developmental cycle of
783 Chlamydia trachomatis. *Proceedings of the National Academy of Sciences of the United*
784 *States of America* **100**, 8478-8483 (2003). https://doi.org/10.1073/pnas.1331135100
785 56 Brockett, M. R. & Liechti, G. W. Persistence alters the interaction between Chlamydia
786 trachomatis and its host cell. *Infect Immun* (2021). https://doi.org/10.1128/IAI.00685-20
787 57 Packiam, M., Weinrick, B., Jacobs, W. R., Jr. & Maurelli, A. T. Structural
788 characterization of muropeptides from *Chlamydia trachomatis* peptidoglycan by mass
789 spectrometry resolves "chlamydial anomaly". *Proceedings of the National Academy of*
790 *Sciences of the United States of America* **112**, 11660-11665 (2015).
791 https://doi.org/10.1073/pnas.1514026112
792 58 Lee, J. K. *et al.* Replication-dependent size reduction precedes differentiation in
793 Chlamydia trachomatis. *Nat Commun* **9**, 45 (2018). https://doi.org/10.1038/s41467-017-
794 02432-0
795 59 Cram, E. D., Rockey, D. D. & Dolan, B. P. Chlamydia spp. development is differentially
796 altered by treatment with the LpxC inhibitor LPC-011. *BMC Microbiol* **17**, 98 (2017).
797 https://doi.org/10.1186/s12866-017-0992-8
798 60 Nguyen, B. D. *et al.* Lipooligosaccharide is required for the generation of infectious
799 elementary bodies in Chlamydia trachomatis. *Proceedings of the National Academy of*
800 *Sciences of the United States of America* **108**, 10284-10289 (2011).
801 https://doi.org/10.1073/pnas.1107478108

802 61 Klockner, A. *et al.* AmiA is a penicillin target enzyme with dual activity in the
803 intracellular pathogen Chlamydia pneumoniae. *Nat Commun* **5**, 4201 (2014).
804 https://doi.org/10.1038/ncomms5201
805 62 Jacquier, N. *et al.* A SpoIID Homolog Cleaves Glycan Strands at the Chlamydial
806 Division Septum. *mBio* **10** (2019). https://doi.org/10.1128/mBio.01128-19
807 63 Adamson, C., Liang, Y., Feng, S., Ng, A. W. R. & Qiao, Y. A closer look at ligand
808 specificity for cellular activation of NOD2 with synthetic muramyl dipeptide analogues.
809 *Chem Commun (Camb)* **60**, 2212-2215 (2024). https://doi.org/10.1039/d3cc05807g
810 64 Ouellette, S. P., Blay, E. A., Hatch, N. D. & Fisher-Marvin, L. A. CRISPR Interference
811 To Inducibly Repress Gene Expression in Chlamydia trachomatis. *Infect Immun* **89**,
812 e0010821 (2021). https://doi.org/10.1128/IAI.00108-21
813 65 Panzetta, M. E., Valdivia, R. H. & Saka, H. A. Chlamydia Persistence: A Survival
814 Strategy to Evade Antimicrobial Effects in-vitro and in-vivo. *Front Microbiol* **9**, 3101
815 (2018). https://doi.org/10.3389/fmicb.2018.03101
816 66 Bavoil, P. M. What's in a word: the use, misuse, and abuse of the word "persistence" in
817 Chlamydia biology. *Front Cell Infect Microbiol* **4**, 27 (2014).
818 https://doi.org/10.3389/fcimb.2014.00027
819 67 Borel, N., Pospischil, A., Hudson, A. P., Rupp, J. & Schoborg, R. V. The role of viable
820 but non-infectious developmental forms in chlamydial biology. *Front Cell Infect*
821 *Microbiol* **4**, 97 (2014). https://doi.org/10.3389/fcimb.2014.00097
822 68 Wyrick, P. B. Chlamydia trachomatis persistence in vitro: an overview. *J Infect Dis* **201**
823 **Suppl 2**, S88-95 (2010). https://doi.org/10.1086/652394
824 69 Workowski, K. A., Lampe, M. F., Wong, K. G., Watts, M. B. & Stamm, W. E. Long-
825 term eradication of Chlamydia trachomatis genital infection after antimicrobial therapy.
826 Evidence against persistent infection. *JAMA* **270**, 2071-2075 (1993).
827 70 Kozusnik, T., Adams, S. E. & Greub, G. Aberrant Bodies: An Alternative Metabolic
828 Homeostasis Allowing Survivability? *Microorganisms* **12** (2024).
829 https://doi.org/10.3390/microorganisms12030495
830 71 Smith, E. P. & Valdivia, R. H. Chlamydia trachomatis: a model for intracellular bacterial
831 parasitism. *J Bacteriol*, e0036124 (2025). https://doi.org/10.1128/jb.00361-24
832 72 O'Connell, C. M., Ionova, I. A., Quayle, A. J., Visintin, A. & Ingalls, R. R. Localization
833 of TLR2 and MyD88 to Chlamydia trachomatis inclusions. Evidence for signaling by
834 intracellular TLR2 during infection with an obligate intracellular pathogen. *J Biol Chem*
835 **281**, 1652-1659 (2006). https://doi.org/10.1074/jbc.M510182200
836 73 Yu, P. *et al.* STAT3-mediated TLR2/4 pathway upregulation in an IFN-gamma-induced
837 Chlamydia trachomatis persistent infection model. *Pathog Dis* **74** (2016).
838 https://doi.org/10.1093/femspd/ftw076
839 74 David, H. L., Takayama, K. & Goldman, D. S. Susceptibility of mycobacterial D-alanyl-
840 D-alanine synthetase to D-cycloserine. *Am Rev Respir Dis* **100**, 579-581 (1969).
841 https://doi.org/10.1164/arrd.1969.100.4.579
842 75 Lambert, M. P. & Neuhaus, F. C. Mechanism of D-cycloserine action: alanine racemase
843 from Escherichia coli W. *J Bacteriol* **110**, 978-987 (1972).
844 https://doi.org/10.1128/jb.110.3.978-987.1972
845 76 Tipper, D. J. & Strominger, J. L. Mechanism of action of penicillins: a proposal based on
846 their structural similarity to acyl-D-alanyl-D-alanine. *Proceedings of the National*

847 *Academy of Sciences of the United States of America* **54**, 1133-1141 (1965).
848 https://doi.org/10.1073/pnas.54.4.1133
849 77 Gulzar, F. *et al.* ER stress aggravates NOD1-mediated inflammatory response leading to
850 impaired nutrient metabolism in hepatoma cells. *Biochem Biophys Res Commun* **735**,
851 150827 (2024). https://doi.org/10.1016/j.bbrc.2024.150827
852 78 Body-Malapel, M. *et al.* NOD2: a potential target for regulating liver injury. *Lab Invest*
853 **88**, 318-327 (2008). https://doi.org/10.1038/labinvest.3700716
854 79 Lyons, J. M., Ito, J. I., Jr., Pena, A. S. & Morre, S. A. Differences in growth
855 characteristics and elementary body associated cytotoxicity between Chlamydia
856 trachomatis oculogenital serovars D and H and Chlamydia muridarum. *J Clin Pathol* **58**,
857 397-401 (2005). https://doi.org/10.1136/jcp.2004.021543
858 80 Kienes, I., Weidl, T., Mirza, N., Chamaillard, M. & Kufer, T. A. Role of NLRs in the
859 Regulation of Type I Interferon Signaling, Host Defense and Tolerance to Inflammation.
860 *Int J Mol Sci* **22** (2021). https://doi.org/10.3390/ijms22031301
861 81 Murray, S. M. & McKay, P. F. Chlamydia trachomatis: Cell biology, immunology and
862 vaccination. *Vaccine* **39**, 2965-2975 (2021).
863 https://doi.org/10.1016/j.vaccine.2021.03.043
864 82 Lupfer, C. *et al.* Receptor interacting protein kinase 2-mediated mitophagy regulates
865 inflammasome activation during virus infection. *Nat Immunol* **14**, 480-488 (2013).
866 https://doi.org/10.1038/ni.2563
867 83 Pachikara, N., Zhang, H., Pan, Z., Jin, S. & Fan, H. Productive Chlamydia trachomatis
868 lymphogranuloma venereum 434 infection in cells with augmented or inactivated
869 autophagic activities. *FEMS Microbiol Lett* **292**, 240-249 (2009).
870 https://doi.org/10.1111/j.1574-6968.2009.01494.x
871 84 Al-Younes, H. M. *et al.* Autophagy-independent function of MAP-LC3 during
872 intracellular propagation of Chlamydia trachomatis. *Autophagy* **7**, 814-828 (2011).
873 https://doi.org/10.4161/auto.7.8.15597
874 85 Yasir, M., Pachikara, N. D., Bao, X., Pan, Z. & Fan, H. Regulation of chlamydial
875 infection by host autophagy and vacuolar ATPase-bearing organelles. *Infect Immun* **79**,
876 4019-4028 (2011). https://doi.org/10.1128/IAI.05308-11
877 86 Waguia Kontchou, C. *et al.* Chlamydia trachomatis inhibits apoptosis in infected cells by
878 targeting the pro-apoptotic proteins Bax and Bak. *Cell Death Differ* **29**, 2046-2059
879 (2022). https://doi.org/10.1038/s41418-022-00995-0
880 87 Sharma, M. & Rudel, T. Apoptosis resistance in Chlamydia-infected cells: a fate worse
881 than death? *FEMS Immunol Med Microbiol* **55**, 154-161 (2009).
882 https://doi.org/10.1111/j.1574-695X.2008.00515.x
883 88 Fan, T. *et al.* Inhibition of apoptosis in chlamydia-infected cells: blockade of
884 mitochondrial cytochrome c release and caspase activation. *The Journal of experimental*
885 *medicine* **187**, 487-496 (1998). https://doi.org/10.1084/jem.187.4.487
886 89 Dean, D. & Powers, V. C. Persistent Chlamydia trachomatis infections resist apoptotic
887 stimuli. *Infect Immun* **69**, 2442-2447 (2001). https://doi.org/10.1128/IAI.69.4.2442-
888 2447.2001
889 90 Henderson, P. & Stevens, C. The role of autophagy in Crohn's disease. *Cells* **1**, 492-519
890 (2012). https://doi.org/10.3390/cells1030492

91 Hamaoui, D. *et al.* The Chlamydia effector CT622/TaiP targets a nonautophagy related function of ATG16L1. *Proceedings of the National Academy of Sciences of the United States of America* **117**, 26784-26794 (2020). https://doi.org/10.1073/pnas.2005389117

92 Tian, D., Cui, M. & Han, M. Bacterial muropeptides promote OXPHOS and suppress mitochondrial stress in mammals. *Cell Rep* **43**, 114067 (2024). https://doi.org/10.1016/j.celrep.2024.114067

93 Noguchi, E., Homma, Y., Kang, X., Netea, M. G. & Ma, X. A Crohn's disease-associated NOD2 mutation suppresses transcription of human IL10 by inhibiting activity of the nuclear ribonucleoprotein hnRNP-A1. *Nat Immunol* **10**, 471-479 (2009). https://doi.org/10.1038/ni.1722

94 Ariffin, J. K. & Sweet, M. J. Differences in the repertoire, regulation and function of Toll-like Receptors and inflammasome-forming Nod-like Receptors between human and mouse. *Curr Opin Microbiol* **16**, 303-310 (2013). https://doi.org/10.1016/j.mib.2013.03.002

95 Magalhaes, J. G. *et al.* Murine Nod1 but not its human orthologue mediates innate immune detection of tracheal cytotoxin. *EMBO Rep* **6**, 1201-1207 (2005). https://doi.org/10.1038/sj.embor.7400552

96 Frohlich, K. M. *et al.* Membrane vesicle production by Chlamydia trachomatis as an adaptive response. *Front Cell Infect Microbiol* **4**, 73 (2014). https://doi.org/10.3389/fcimb.2014.00073

97 Harned, R. L., Hidy, P. H. & La Baw, E. K. Cycloserine. I. A preliminary report. *Antibiot Chemother (Northfield)* **5**, 204-205 (1955).

98 Epstein, I. G., Nair, K. G. & Boyd, L. J. Cycloserine, a new antibiotic, in the treatment of human pulmonary tuberculosis: a preliminary report. *Antibiotic Med Clin Ther (New York)* **1**, 80-93 (1955).

99 Prosser, G. A. & de Carvalho, L. P. Kinetic mechanism and inhibition of Mycobacterium tuberculosis D-alanine:D-alanine ligase by the antibiotic D-cycloserine. *FEBS J* **280**, 1150-1166 (2013). https://doi.org/10.1111/febs.12108

100 De Benedetti, S. *et al.* Characterization of serine hydroxymethyltransferase GlyA as a potential source of D-alanine in Chlamydia pneumoniae. *Front Cell Infect Microbiol* **4**, 19 (2014). https://doi.org/10.3389/fcimb.2014.00019

101 Stephens, R. S. *et al.* Genome sequence of an obligate intracellular pathogen of humans: Chlamydia trachomatis. *Science* **282**, 754-759 (1998). https://doi.org/10.1126/science.282.5389.754

102 Girardin, S. E. *et al.* Peptidoglycan molecular requirements allowing detection by Nod1 and Nod2. *J Biol Chem* **278**, 41702-41708 (2003). https://doi.org/10.1074/jbc.M307198200

103 Kuru, E. *et al.* Mechanisms of Incorporation for D-Amino Acid Probes That Target Peptidoglycan Biosynthesis. *ACS Chem Biol* **14**, 2745-2756 (2019). https://doi.org/10.1021/acschembio.9b00664

104 Sun, H. S. *et al.* Chlamydia trachomatis vacuole maturation in infected macrophages. *J Leukoc Biol* **92**, 815-827 (2012). https://doi.org/10.1189/jlb.0711336

105 Al-Zeer, M. A., Al-Younes, H. M., Lauster, D., Abu Lubad, M. & Meyer, T. F. Autophagy restricts Chlamydia trachomatis growth in human macrophages via IFNG-inducible guanylate binding proteins. *Autophagy* **9**, 50-62 (2013). https://doi.org/10.4161/auto.22482

937 106 Faustin, B. *et al.* Reconstituted NALP1 inflammasome reveals two-step mechanism of
938 caspase-1 activation. *Mol Cell* **25**, 713-724 (2007).
939 https://doi.org/10.1016/j.molcel.2007.01.032
940 107 Yang, C. *et al.* Chlamydia evasion of neutrophil host defense results in NLRP3 dependent
941 myeloid-mediated sterile inflammation through the purinergic P2X7 receptor. *Nat*
942 *Commun* **12**, 5454 (2021). https://doi.org/10.1038/s41467-021-25749-3
943

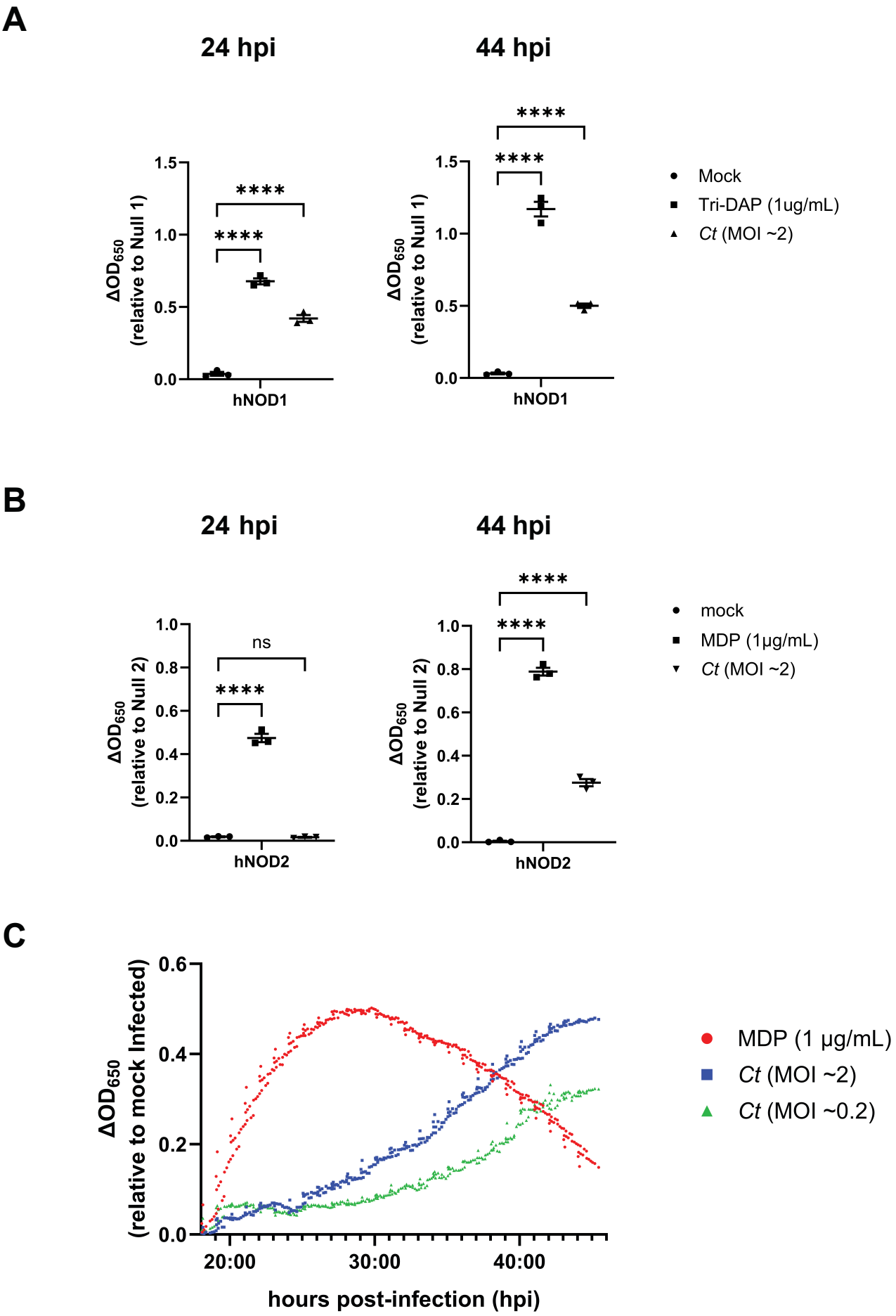
A
24 hpi
44 hpi
****
****
****
****
1.5
1.0
0.5
0.0
ΔOD650
(relative to Null 1)
hNOD1
Mock
Tri-DAP (1ug/mL)
Ct (MOI ~2)
B
24 hpi
44 hpi
ns
****
****
****
1.0
0.8
0.6
0.4
0.2
0.0
ΔOD650
(relative to Null 2)
hNOD2
mock
MDP (1µg/mL)
Ct (MOI ~2)
C
0.6
0.4
0.2
0.0
ΔOD650
(relative to mock Infected)
20:00
30:00
40:00
hours post-infection (hpi)
MDP (1 µg/mL)
Ct (MOI ~2)
Ct (MOI ~0.2)

A

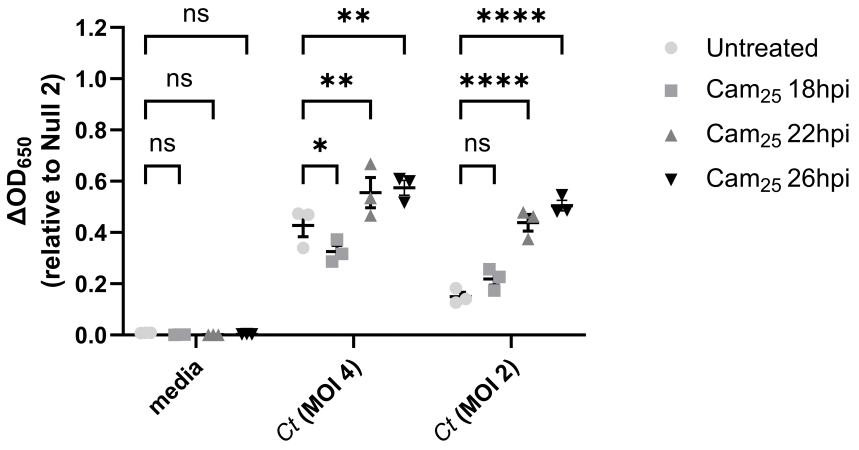
ΔOD650 (relative to Null 2)
1.2
1.0
0.8
0.6
0.4
0.2
0.0
ns
ns
ns
**
**
*
****
****
ns
media
Ct (MOI 4)
Ct (MOI 2)
Untreated
Cam25 18hpi
Cam25 22hpi
Cam25 26hpi

B

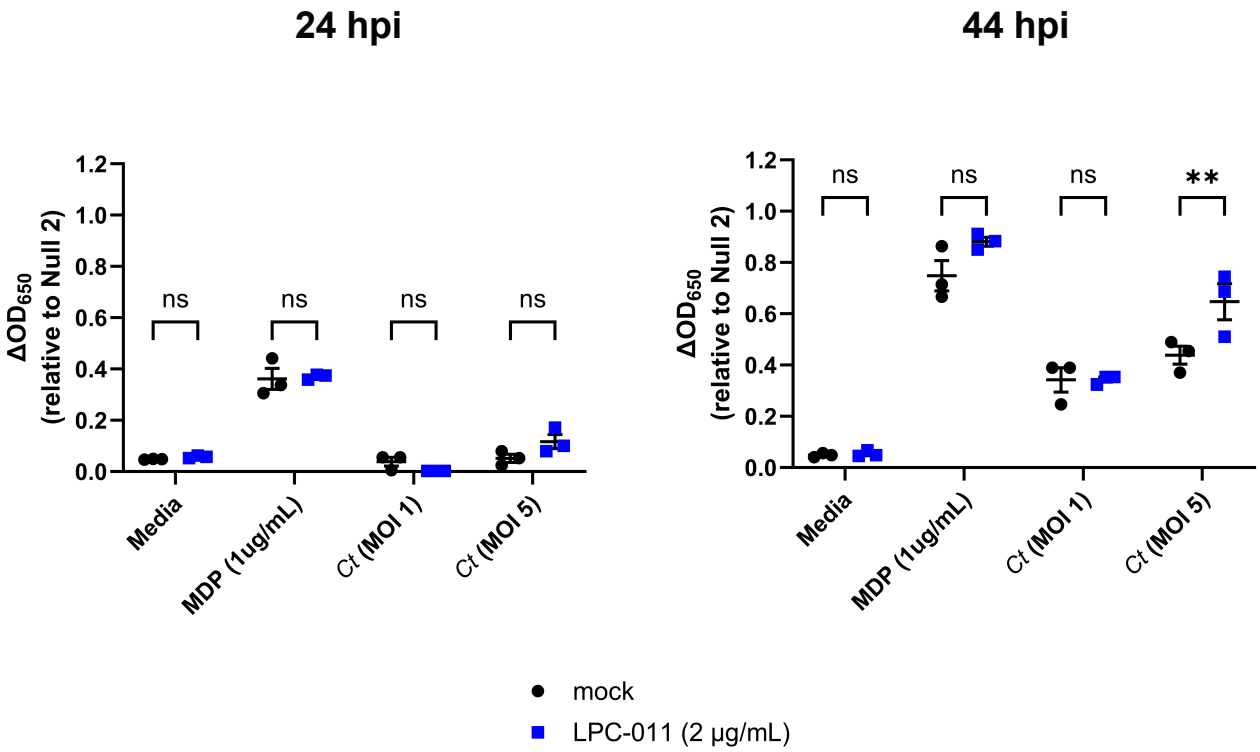
24 hpi
44 hpi
ΔOD650 (relative to Null 2)
1.2
1.0
0.8
0.6
0.4
0.2
0.0
ns
ns
ns
ns
ns
ns
ns
**
Media
MDP (1ug/mL)
Ct (MOI 1)
Ct (MOI 5)
mock
LPC-011 (2 µg/mL)

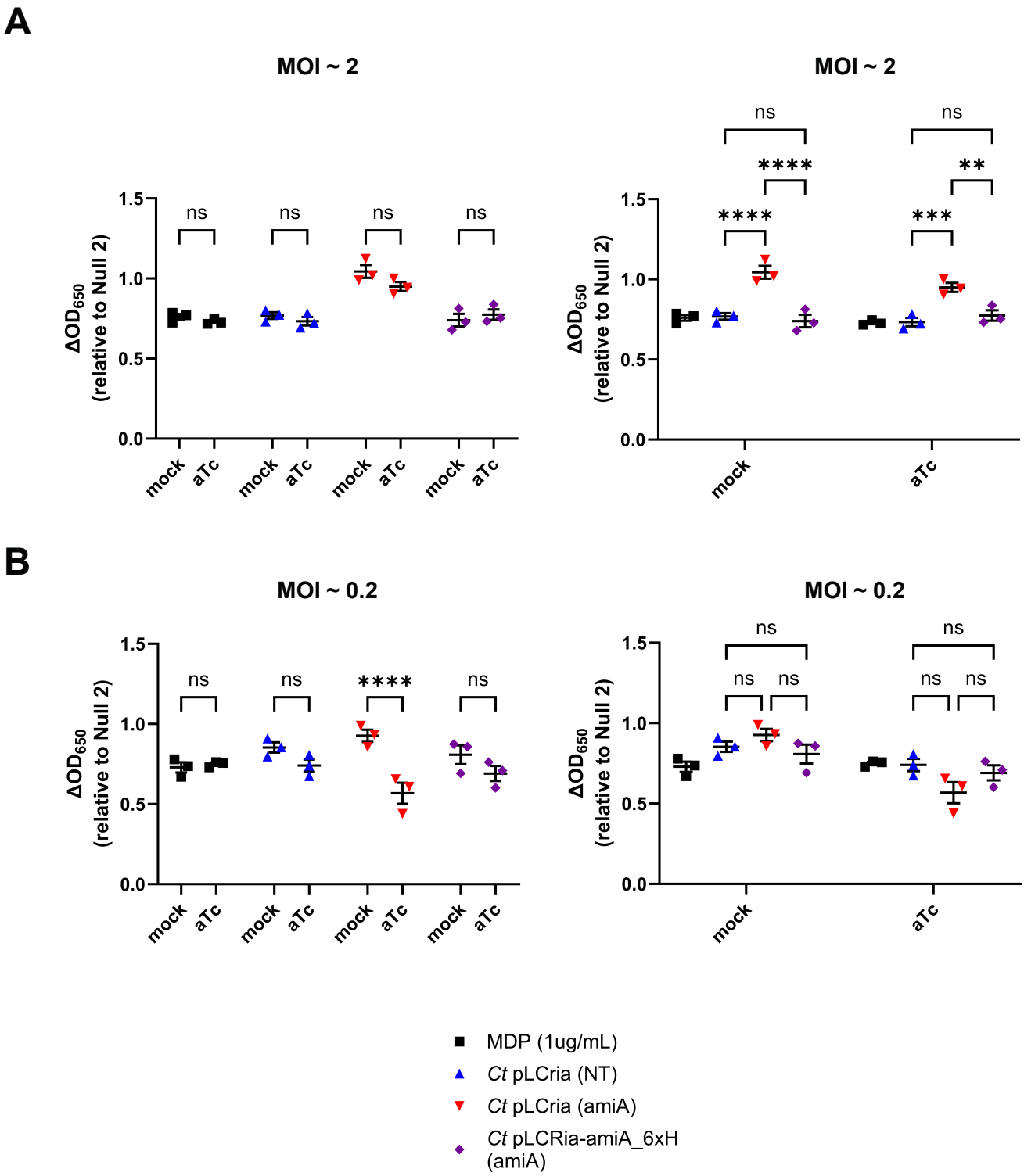
A
MOI ~ 2
MOI ~ 2
ΔOD650 (relative to Null 2)
1.5
1.0
0.5
0.0
ns
****
**
***
mock
aTc
B
MOI ~ 0.2
MOI ~ 0.2
MDP (1ug/mL)
Ct pLCria (NT)
Ct pLCria (amiA)
Ct pLCRia-amiA_6xH (amiA)

A

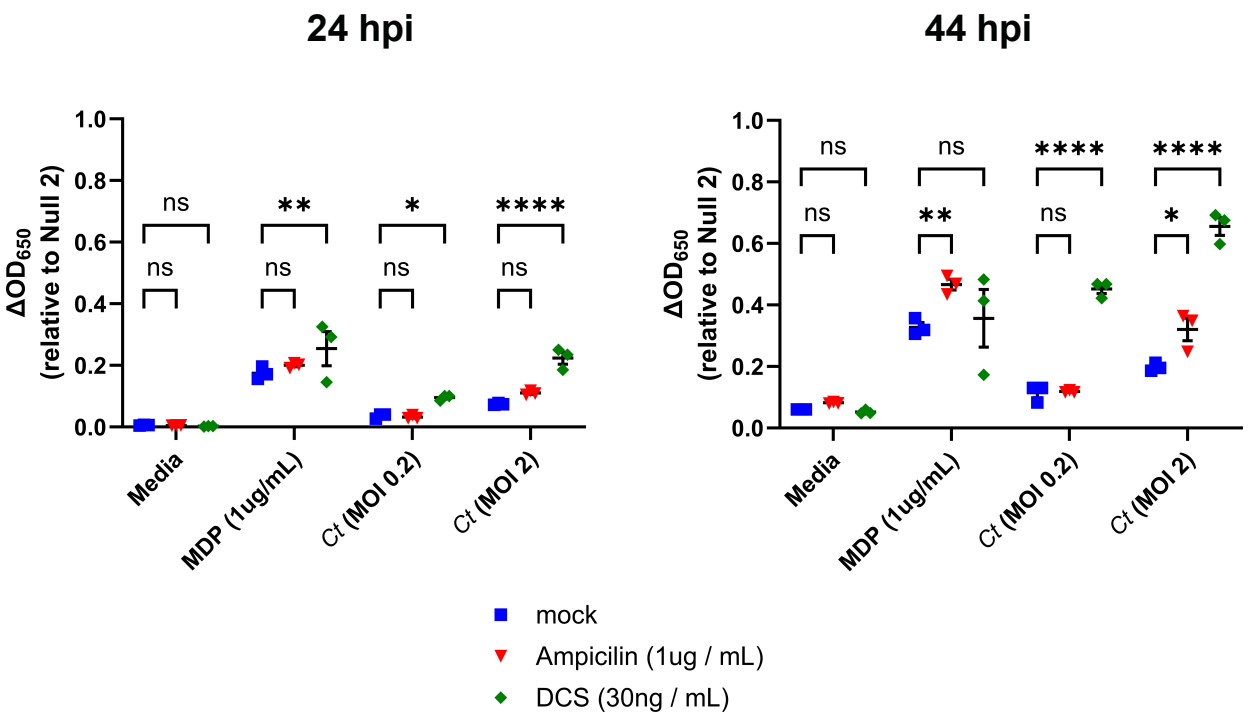
24 hpi
44 hpi
ΔOD650 (relative to Null 2)
1.0
0.8
0.6
0.4
0.2
0.0
ns
**
*
****
Media
MDP (1ug/mL)
Ct (MOI 0.2)
Ct (MOI 2)
mock
Ampicilin (1ug / mL)
DCS (30ng / mL)

B

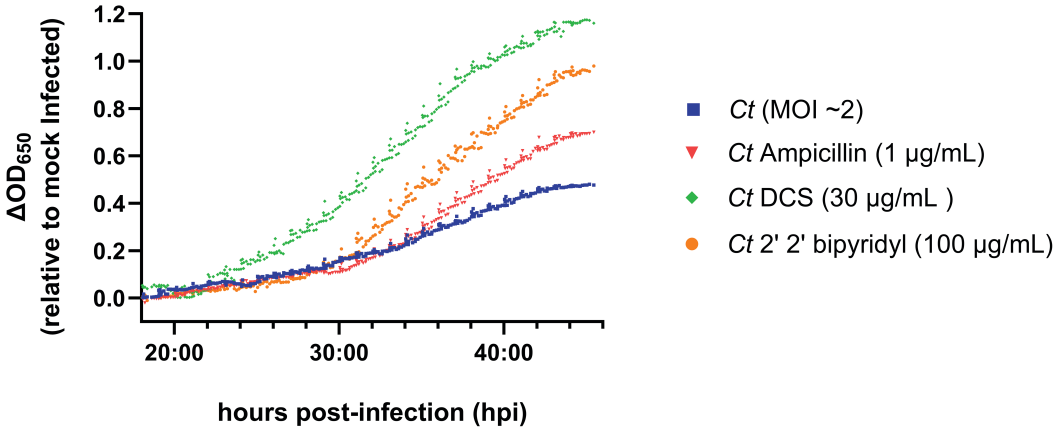
ΔOD650 (relative to mock Infected)
1.2
1.0
0.8
0.6
0.4
0.2
0.0
20:00
30:00
40:00
hours post-infection (hpi)
Ct (MOI ~2)
Ct Ampicillin (1 µg/mL)
Ct DCS (30 µg/mL)
Ct 2' 2' bipyridyl (100 µg/mL)

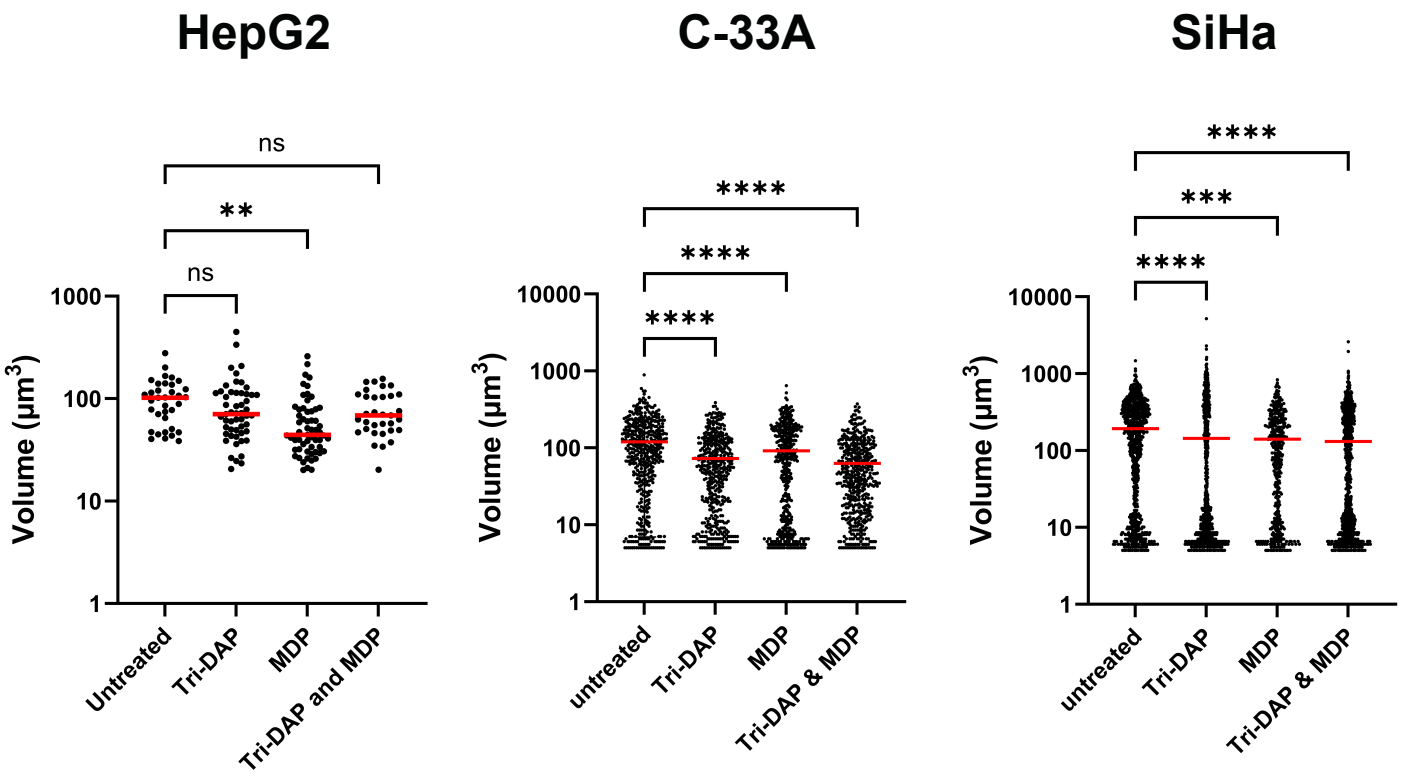
HepG2
C-33A
SiHa
ns
**
ns
****
****
****
****
***
****
Volume (µm3)
1000
100
10
1
10000
1000
100
10
1
10000
1000
100
10
1
Untreated
Tri-DAP
MDP
Tri-DAP and MDP
untreated
Tri-DAP
MDP
Tri-DAP & MDP
untreated
Tri-DAP
MDP
Tri-DAP & MDP

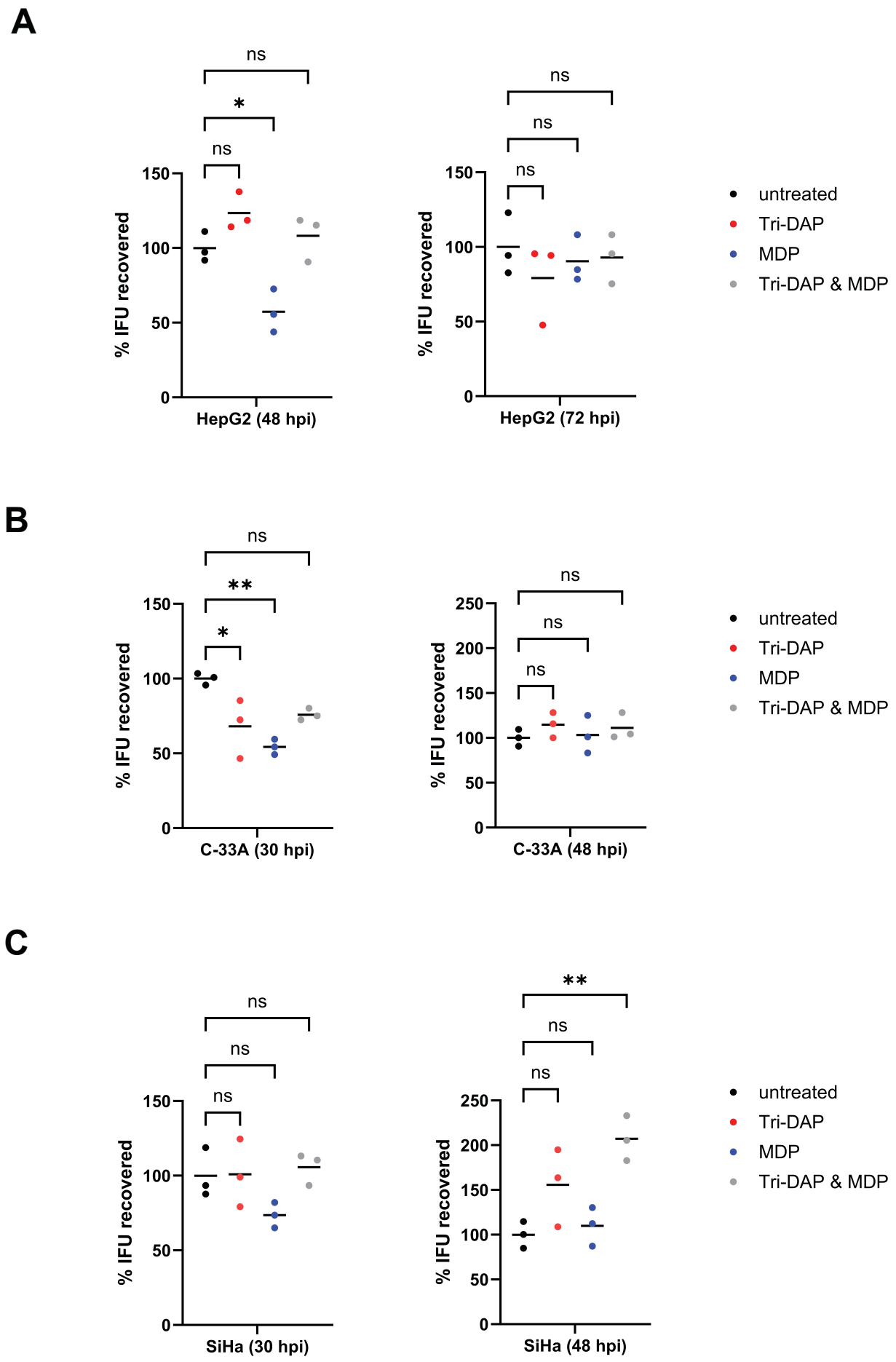
A
ns
*
ns
150
100
50
0
% IFU recovered
HepG2 (48 hpi)
ns
ns
ns
150
100
50
0
% IFU recovered
HepG2 (72 hpi)
untreated
Tri-DAP
MDP
Tri-DAP & MDP
B
ns
**
*
150
100
50
0
% IFU recovered
C-33A (30 hpi)
ns
ns
ns
250
200
150
100
50
0
% IFU recovered
C-33A (48 hpi)
untreated
Tri-DAP
MDP
Tri-DAP & MDP
C
ns
ns
ns
150
100
50
0
% IFU recovered
SiHa (30 hpi)
**
ns
ns
250
200
150
100
50
0
% IFU recovered
SiHa (48 hpi)
untreated
Tri-DAP
MDP
Tri-DAP & MDP

A

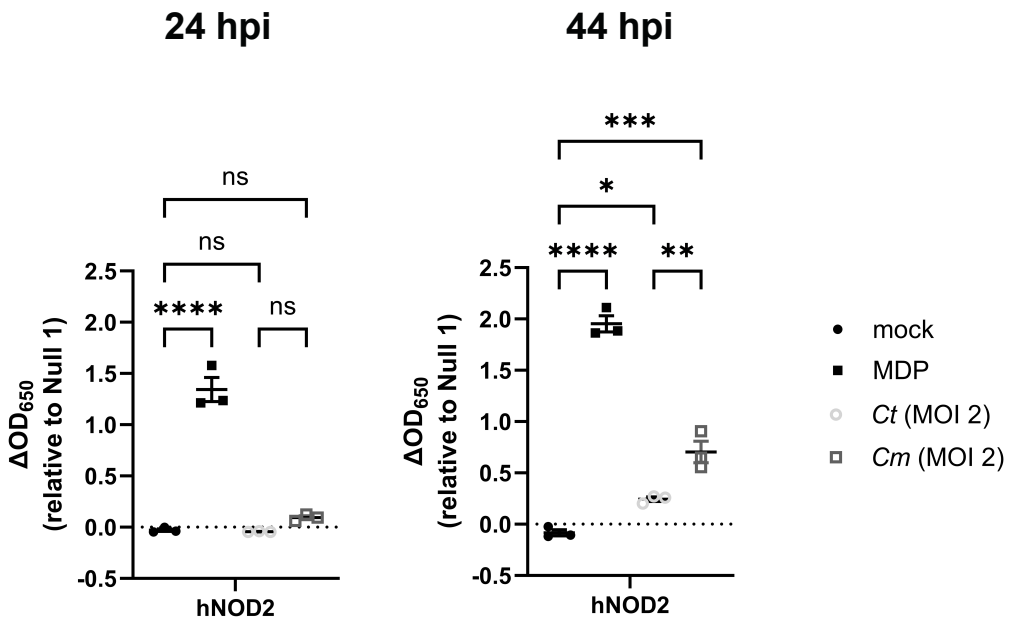
24 hpi
44 hpi
ΔOD650 (relative to Null 1)
hNOD2
ns
****
*
**
***
mock
MDP
Ct (MOI 2)
Cm (MOI 2)

B

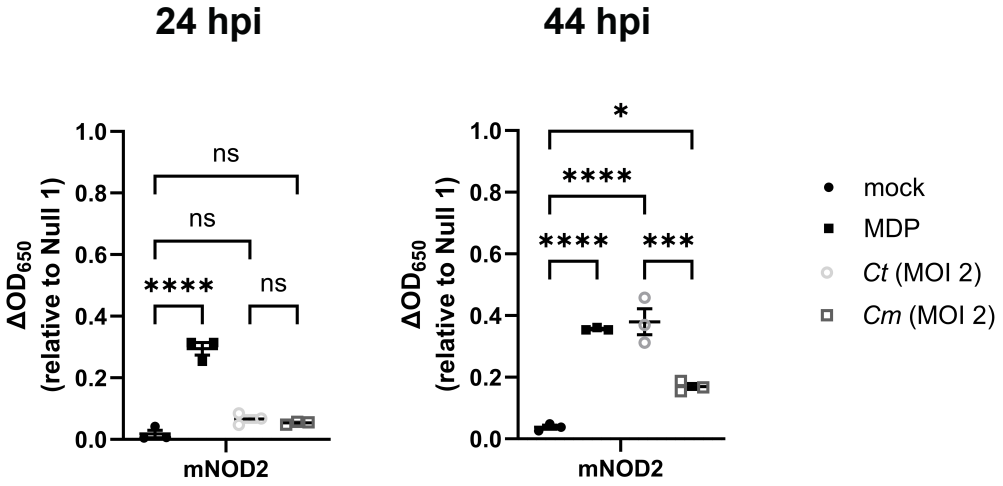
24 hpi
44 hpi
ΔOD650 (relative to Null 1)
mNOD2
ns
****
*
***
mock
MDP
Ct (MOI 2)
Cm (MOI 2)

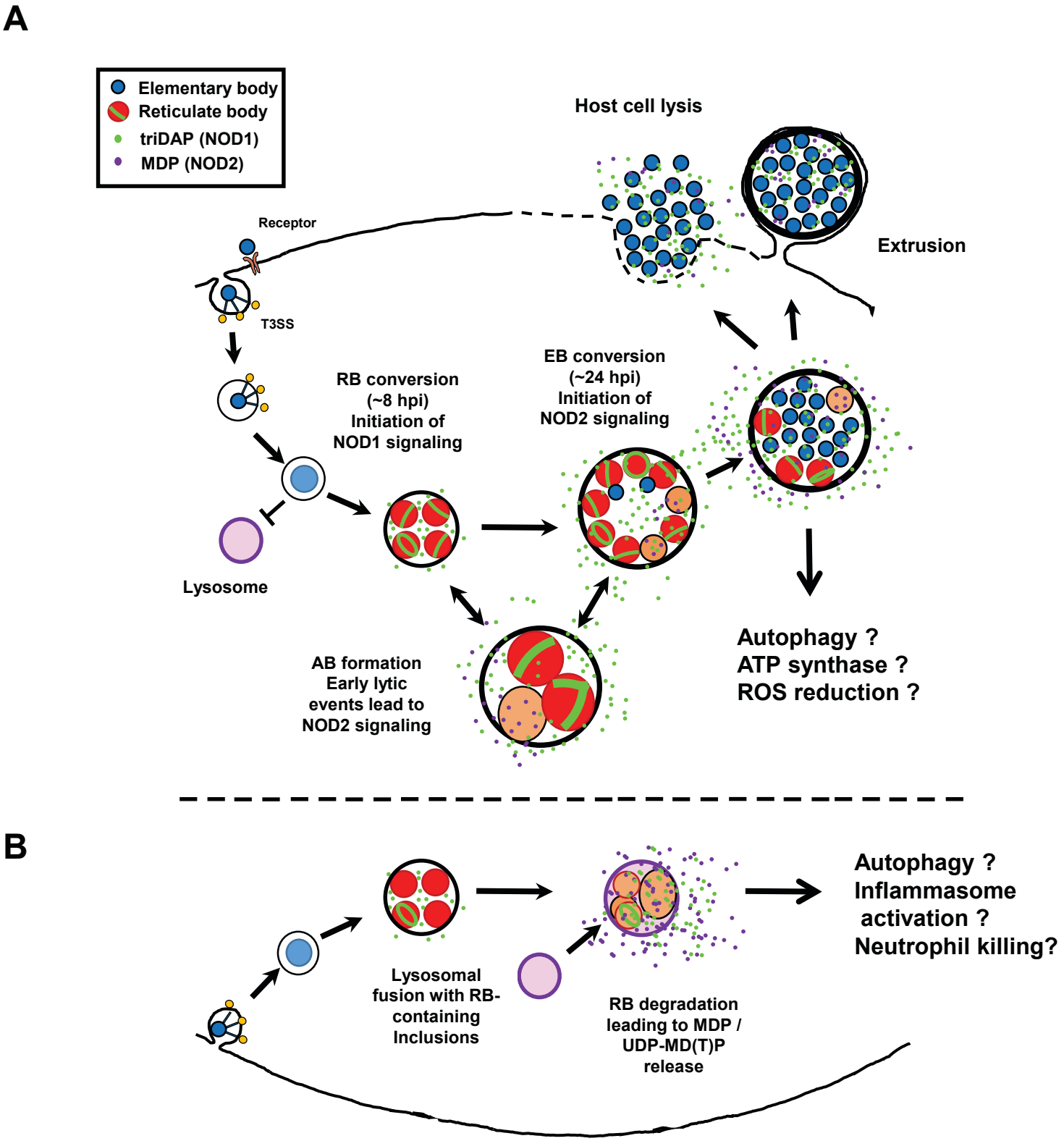
A
Elementary body
Reticulate body
triDAP (NOD1)
MDP (NOD2)
Host cell lysis
Extrusion
Receptor
T3SS
RB conversion
(~8 hpi)
Initiation of
NOD1 signaling
EB conversion
(~24 hpi)
Initiation of
NOD2 signaling
Lysosome
AB formation
Early lytic
events lead to
NOD2 signaling
Autophagy ?
ATP synthase ?
ROS reduction ?
B
Lysosomal
fusion with RB-
containing
Inclusions
RB degradation
leading to MDP /
UDP-MD(T)P
release
Autophagy ?
Inflammasome
activation ?
Neutrophil killing?